

A graph-based search approach for planning and learning

An application to planar pushing and navigation tasks

SC52045: System & Control Thesis Report

G.S. Groote

page intentionally left blank.

A graph-based search approach for planning and learning

An application to planar pushing and navigation tasks

by

G.S. Groote

Student Name Student Number

Gijs S. Groote 4483987

Supervisors: C. Smith, M. Wisse

Daily Supervisor: C. Pezzato

Project Duration: Nov, 2021 - Feb, 2023

Faculty: Faculty of Cognitive Robotics, Delft

Cover: Simulation environment used during the thesis [33].

Style: TU Delft Report Style, with modifications by Daan Zwaneveld



Delft Center for
Systems and Control



Cognitive
Robotics

Abstract

In the field of robotics, much attention has been given to the research topics *learning object dynamics* [6, 32], *Navigation Among Movable Objects (NAMO)* [5, 10, 17, 20] and *nonprehensile pushing* [2, 3, 21, 34, 35, 36]. However, because scientific papers that include all three topics are scarce, the combination of these research topics into one robot framework has not been explored sufficiently. A combination of the topics leads to an improvement in planning, faster execution times and rapidly concluding unfeasibility for a robot acting in new and unforeseen environments.

To solve the problem presented in the first paragraph, this thesis proposes a robot framework that combines these three research topics. This framework comprises of three key components: the **hypothesis algorithm**, the **hypothesis graph**, and the **knowledge graph**. The hypothesis algorithm is used to draw a hypothesis on how to relocate an object to a new pose by computing possible action sequences given certain robot skills. In doing so, the hypothesis algorithm creates an hypothesis graph that encapsulates the structure of the action sequences and ensures the robot eventually halts. Once an hypothesis is carried out on the robot, information about the execution, such as the outcome, the type of controller used and other metrics, are stored in the knowledge graph. The knowledge graph is populated over time, allowing the robot to learn, for instance, object properties and then refine the hypothesis to increase task performance, such as success rate and execution time.

The hypothesis algorithm relies on planning to generate hypotheses, for the purpose of planning and freeing blocked paths that can be encountered, a new planning algorithm is proposed. This planner extends the double tree optimised Rapidly-exploring Random Tree algorithm [5]. The planners both construct a configuration space for an object and are provided with starting and target pose for that object. The planners then convert these poses to points in configuration space and searches for a path connecting the starting point to the target point. A key difference between the newly proposed planner and the existing planner lies in the ability to detect blocked paths. For the new planner, objects are initially classified as “unknown” and can later be categorized as either “movable” or “obstacle”. The object type information is then used when constructing the configuration space for the newly proposed planning algorithm. Its configuration space consists of the conventional free, obstacle, and unknown-and movable space.

To carry out the investigation, a mobile robot in a robot environment is created with movable and unmovable objects. The robot is given a task that involves relocating a subset of the objects in the robot environment through driving and nonprehensile pushing. The task can be broken down into individual subtasks that consist of an object and a target pose. Planning for a push or drive action occurs with the newly proposed planning algorithm that, if successful, provides a path that can be tracked.

The three topics can be combined into a robot framework because results indicate that task execution improves as the robot gains more experience in its environment. The proposed framework, which covers all three research topics, performs equivalent or better compared to the state-of-the-art frameworks that are specialized in only two out of three research topics [11, 30, 31, 38, 40].

G.S. Groote
Delft, May 2023

Contents

Abstract	i
Symbols	v
1 Introduction	1
1.1 Research Question	6
1.2 Problem Description	6
1.2.1 Task Specification	7
1.2.2 Assumptions	7
1.2.3 An Example of Robots and Objects	8
1.3 Report Structure	9
2 Required Background	10
2.1 System Identification	10
2.2 Control Methods	11
2.3 Planning	11
2.3.1 Estimating Path Existence	12
2.3.2 Motion Planning	15
2.3.3 Manipulation Planning	22
2.4 Monitoring Metrics	22
3 The Hypothesis and Knowledge Graph	24
3.1 Hypothesis Graph	26
3.1.1 Definition	27
3.1.2 Hypothesis Algorithm	30
3.1.3 The Search and the Execution Loop	35
3.1.4 Examples	36
3.2 Knowledge Graph	41
3.2.1 Definition	41
3.2.2 Example	42
3.2.3 Edge Metrics	43
4 Results	45
4.1 Proposed Method Metrics	45
4.2 Randomization	47
4.3 Comparison with State-of-the-Art	52
5 Conclusions	56
5.1 Future work	57
5.1.1 Removing Assumptions	57
Glossary	59
References	60
6 Appendix	64
A Complexity Classes	65
B Control Methods	66
B.1 Model Predictive Control (MPC) Control	66
B.2 Model Predictive Path Integral (MPPI) Control	68

List of Figures

1.1	Two robots in the simulation environment	8
1.2	Two objects in the robot environment	9
2.1	Environment with the point robot, unmovable yellow walls and movable brown boxes. The robot classifies all objects as unknown since it is unaware of the objects' classes.	14
2.2	The configuration space for the point robot with different cell sizes. The robot environment corresponds to the environment presented in Figure 2.1.	14
2.3	Visualization of the Double tree RRT* motion planner that adds a single sample to the connectivity graph. The colour of the box surrounding subfigures corresponds to the coloured sections in Algorithm 1. 3-dimensional configuration space displayed as 2-dimensional configuration space (x and y are visible, θ is not visible).	19
2.4	Comparing schematic example to a visualization of the real algorithm.	20
2.5	The robot tasked with driving toward the other side of the brown box.	21
2.6	Generating a new robot configuration whilst adding a sample to the connectivity tree during manipulation planning.	22
3.1	Flowchart representation of the proposed framework.	24
3.2	FSM displaying the status of an identification edge	28
3.3	FSM displaying the status of an action edge	29
3.4	Flowchart displaying the hypothesis graph's workflow.	33
3.5	The search (above) and execution (below) loop.	35
3.6	Legend for hypothesis graph (hgraph)'s nodes and edges	36
3.7	hgraph generated by the hypothesis algorithm (halgorithm) to drive the robot to a target configuration	36
3.8	Executing the hypothesis found in Figure 3.7.	37
3.9	hgraph for pushing the green box to the target configuration	38
3.10	hgraph for driving to target configuration and encountering a blocked path	39
3.11	Executing two hypothesis, both failing to complete because a fault of failure emerged.	40
3.12	knowledge graph (kgraph) with 3 edges on robot driving, and 2 edges for pushing the green box.	43
4.1	Two random environments with 2 target ghost configurations for the task containing 2 subtasks.	48
4.2	A random environment that is reshuffled 4 times. Target ghost configurations are not shown.	48
4.3	Robot tasked to drive toward 3 target configurations, the environment is reshuffled after completing a task.	49
4.4	Execution times for driving toward target configurations with and without kgraph.	50
4.5	Average Prediction Error and Standard Deviation for action edges during a pushing task.	51
4.6	Planning times for pushing an object toward the target a configuration.	51
4.7	Execution times for pushing an object to target configurations with and without kgraph.	52
B.1	System $G(t)$ with input $u(t)$, output $y(t)$ and MPC controller with input $y(t)$, reference signal $y_{ref}(t)$, parameterisation p and constraint sets $\mathbb{X}, \mathbb{U}, \mathbb{Y}$	66
B.2	A discrete MPC scheme tracking a constant reference signal. k indicates the discrete time step, N the control horizon	68
B.3	MPPI controlled race car using a control horizon of 3 time steps, with 3 rollouts all having their respected inputs as $u_{i,j}$ where i is the rollout index and j indicates the time step [22].	69

List of Tables

1.1	Overview of topics; learning object dynamics, NAMO and specifying target poses in recent literature. This thesis combines the three topics; learning object dynamics, NAMO and nonprehensile pushing.	6
2.1	Functions used by the Algorithm 1	17
2.2	Monitor metrics used to monitor if a fault occurred during the execution of an edge	23
3.1	Terminology of terms used	26
3.2	Functions used by the Algorithm 1	31
3.3	Elaborate information on actions taken by blocks in Figure 3.4.	34
3.4	Edge metrics used to rank control methods from ‘good’ to ‘bad’	44
4.1	Proposed method metrics used to compare the proposed framework with the state-of-the-art.	46
4.2	Available drive and push system models used for testing.	46
4.3	Overview of recent state-of-the-art papers that include a subset of the 3 topics (learning system models, NAMO, and nonprehensile pushing). The <i>grasp-push</i> and <i>grasp-pull</i> refer to prehensile push and pull manipulation, <i>gripped</i> refers to fully gripping and lifting objects for manipulation, <i>pushing</i> refers to nonprehensile push manipulation. The test metric indicates the testing method used by the paper, where the underlined metric is used to compare against the proposed framework.	53

Symbols

\mathbb{R}	Set of Real numbers
$\mathbb{Z}_{\geq 0}$	Set of non-negative integers
n	Number of Degrees Of Freedom
obj	Object in the robot environment
Obj	Set of objects
m	Number of objects in the environment
Origin	Origin of the environment with with x (north to south), y (west to east) and z (down to up) axis
Ground Plane	The robot environment ground plane
Eq	Set of motion equations in the robot environment
k	time step index
ϵ^{pred}	Prediction Error
ϵ^{track}	Tracking Error
C-space	Configuration Space, $Dim(\text{C-space}) \in \mathbb{R}^2 \vee \mathbb{R}^3$
c	Configuration, point in configuration space
\hat{c}	Estimated configuration
x	distance to Origin over the x -axis
y	distance to Origin over the y -axis
θ	angular distance toward the the Origin's positive x -axis around the z axis
x_{grid}	length of grid in direction of x -axis
y_{grid}	length of grid in direction of y -axis
s_{cell}	length and width of a cell
v	Node in motion or manipulation planner
V_{MP}	Set of nodes for motion or manipulation planner
E_{MP}	Set of edges for motion or manipulation planner
P	Set of paths
S	Task, Tuple of objects and corresponding target configurations.
s	subtask, tuple of an object and an target configuration
h	hypothesis, Sequence of successive edges in the hypothesis graph, an idea to put a object at it's target configuration
$G^{hypothesis}$	hypothesis graph
$G^{knowledge}$	knowledge graph

v	Node in hypothesis or knowledge graph
V_H	Set of nodes for hgraph
V_K	Set of nodes for kgraph
e	Edge hypothesis or knowledge graph
E_H	Set of edges for hgraph
E_K	Set of edges for kgraph
NODE_STATUS	Status of a node
EDGE_STATUS	Status of a edge
OBJ_CLASS	classification of an object
ob	observation from the robot environment
α	Success factor for an edge in kgraph

1

Introduction

This chapter narrows the broad field of robotics down to a largely unsolved problem, combining the three topics; learning object dynamics, NAMO and nonprehensile pushing. For that problem, state-of-the-art methods are presented, and their shortcomings are highlighted in the upcoming paragraphs. Then the gap in literature regarding the combination of the aforementioned topics is summarized in Section 1.1 in the form of the main and sub-research questions. The combination of the three topics is then narrowed down to the scope of this thesis in the problem description, Section 1.2. The chapter finishes by presenting all upcoming chapters in the report structure, Section 1.3.

For robots, navigating and acting in new, unseen environments remains a complicated problem. From the emerged challenges robots face in such environments, three topics are selected, namely: **learning object dynamics**, **Navigation Among Movable Objects (NAMO)** and **nonprehensile pushing**. The main goal of this thesis is to combine these three topics. A secondary goal is to investigate how these topics can strengthen each other over time. When investigating the influence of the topics on each other, questions arise, such as: How does learned environmental knowledge influence planning? Does the execution time decrease, and how much for a repeated task? How much can generated action sequences improve as the robot learns more?

Learning object dynamics enables the robot to manipulate unforeseen objects, NAMO allows the robot to move around in an environment even if an object blocks the robot's target location, and nonprehensile pushing allows the robot to change the environment. Combining these three topics covers any task that involves relocating objects by pushing, which is a wide variety of tasks. Learning abilities allow robots to operate in new environments and to adapt to environmental changes. Examples are exploration, rescue missions or construction sites. An unfamiliar environment can emerge by slightly changing a familiar environment, such as a supermarket with people. Learning abilities are crucial when the robot can encounter many different objects.

Navigation Among Movable Objects can be described as; the robot having to navigate to a goal pose in an unknown environment that consists of static and movable objects. The robot may move objects if the goal can not be reached otherwise or if moving the object may significantly shorten the path to the goal [12].

Nonprehensile pushing is a form of manipulation widely available for robots, even though they are not intentionally designed for pushing. Mobile robots can drive (and thus push) against objects, and a robot arm with a gripper can push against objects even if the gripper is already full. Many robots can push, which is a manipulation action many robots should leverage.

The NAMO problem and nonprehensile pushing are overlapping topics. Moving an object out of the way to free a path (NAMO) is similar to pushing an object to a target pose. However, by combining both topics, a new situation may occur. When pushing obj_a to a new pose, the path is blocked by obj_b which must thus first be moved. When pushing obj_b to a new pose, the path is blocked by obj_c , which must

thus first be moved, etc. Such a situation will not occur when dealing with only the NAMO problem or with only nonprehensile pushing. A robot that can place an object at new poses on top of NAMO can handle a broader variety of tasks compared to a robot that can only navigate among movable objects.

Research into approaches tackling the three topics just described can be split into two categories. The bulk falls into the category of hierarchical approaches [11, 19, 31, 38, 40]. The remainder falls in category locally optimal approaches [23, 29, 30]. Both approaches are elaborated upon later in this chapter. First, the configuration space that builds up to the composite configuration space is discussed. Then secondly, two challenges are highlighted that are related to the composite configuration space growth of dimension and the fact that the composite configuration space is piecewise-analytic.

Configuration Space Now planning for a single action and its relation to the configuration space are investigated. Finding a path for a single action (such as robot driving or robot pushing) is known as a *motion- or manipulation planning problem* and is planned in configuration space. *Configuration space* for an object obj can be described as an n -dimensional space, where n is the number of degrees of freedom for that single object obj . A point in this n -dimensional configuration space fully describes where that object is in the workspace. Then the workspace obstacles are mapped to configuration space to indicate for which configurations the object obj is in collision with an obstacle in the workspace. The subset of configurations in configuration space for which obj is in a collision is called *obstacle space*. The remainder of obstacle space subtracted from configuration space is free space, in which the object can move freely. For every object in the environment, a configuration space can be constructed. A mathematical configuration space description can be found in Section 2.3.1. When a configuration space is constructed, dedicated path planners leverage the configuration space to determine if a configuration lies in free or obstacle space.

Composite Configuration Space Planning for an action sequence and its relation to the composite configuration space is investigated. For a robot environment that involves relocating objects among the presence of other movable objects planning for a single action is not enough because manipulating an object directly to a target position is, in many cases, unfeasible. For example, manipulating an object obj_A to a target position is feasible if the object obj_B that blocks that path is first removed. Clearly, removing blocking object obj_B influences the feasibility of manipulating obj_A to its target position. For planning, there must be a connection between the configuration space of obj_A and obj_B , where the composite configuration space emerges. A *composite configuration space* or composite space emerges when an object's configuration space is augmented with the configuration space of other objects [37]. A composite configuration in such a composite space fully describes where the robot and objects are in the workspace. In recent literature, the composite configuration space is also named composite configuration space [38], finding “bridges” between configuration spaces [13] or room configuration [30]. The term composite configuration space has been selected because it indicates multiple configuration spaces composed together and does not confuse with robot joints (or hinges). Path planners (in contrast to the planning in configuration space) have great difficulty in connecting a starting composite configuration to a target composite configuration [28] for reasons that are discussed in the upcoming paragraph.

Challenges Three challenges are now listed, two related to planning in composite space and one due to unknown environments. The first challenge is that the composite configuration space grows exponentially with the number of movable objects in the environment. The dimension of a robot environment’s composite configuration space can be written as:

$$m_{\text{composite}}^{\text{env}} = \sum_{obj \in Obj | \text{OBJ_CLASS}=\text{movable}} m_{\text{configuration}}^{obj}$$

Thus the dimension of the composite space grows linearly with the number of objects in the robot environment, and the composite configuration space itself grows exponentially, also known as the *curse of dimensionality*.

The second challenge is due to constraint sets. In configuration space, a single constraint set applies that originates from constraints. For example, from a nonholonomic robot, the class of robots that can be described by a bicycle model [25] are nonholonomic. These robots, such as the boxer robot in Figure 1.1b, cannot drive sideways. The nonholonomic constraints must be respected during planning for the path planner to yield feasible paths. Only a single constraint set exists in configuration space, also called *mode of dynamics* [13], because configuration space relates to a single action. Dedicated path planners such as PRM [14], PRM*, RRT or RRT* [15] can find paths in configuration space whilst respecting the constraint set and guarantee asymptotic optimality [15]. In composite space, multiple modes of dynamics exist; the composite configuration must respect the constraints set of the mode of dynamics it resides in. These different modes of dynamics make the composite configuration space *piecewise-analytic*. Path planners have great difficulty crossing the boundary from one mode of dynamics to another mode of dynamics [38].

Appendix A explains complexity classes which may be helpful in understanding this paragraph better. Finding an optimal action sequence to a NAMO and nonprehensile pushing problem requires a search in composite space. Due to the challenges described above, such a problem falls in the category of non-deterministic polynomial-time hard (NP-hard) problems, for which we now provide a reduction. If the search for an optimal solution in composite configuration space is simplified by completely removing relocating objects to new positions from the task, a purely NAMO problem is what remains. Suppose the problem is simplified even further by assuming that every object is an unmoving obstacle. In that case, the problem falls in the category of NP-hard problems because a reduction exists from the piano mover’s problem, which is known to be NP-hard [27]. That a simplified version is NP-hard indicates the difficulty of finding an optimal path in composite configuration space.

The search for an optimal solution in composite space is unthinkable, no recent literature actually plans directly into composite space. Significant simplifications are applied to the composite space, which will be discussed in the next paragraph. Finding paths for multiple actions without opting for an optimal solution, also known as multi-model planning [13], can be achieved using one of the two methods. The first method connects multiple configuration spaces, *hierarchical approaches*, and the second method introduces simplifications to the composite configuration space that allow finding a path, *locally optimal approaches*.

The last challenge introduced is the uncertainty of actions in unknown environments. Planning an action sequence with limited or no environmental knowledge inevitably leads to unfeasible action sequences, such as pushing unmoving obstacles. Updating the environmental knowledge and replanning the action sequence is the cure to the uncertainty introduced by a lack of environmental knowledge. Trying to complete unfeasible action sequences is time and resources lost. Additionally, it can lead to the task itself becoming unfeasible. For example, a pushing robot pushes an object into a dead end due to an action sequence planned with limited environmental knowledge. Now that the object is stuck, the task has become unfeasible.

To summarise, the main challenge is to *find an action sequence for a given task to relocate objects that consist of push and drive actions in new and unforeseen environments*. A search cannot be performed in the composite configuration space because it would require solving an NP-hard problem due to two reasons. First, the composite space grows exponentially with the number of movable objects. Secondly, the composite configuration space piecewise-analytic path planners have great difficulty crossing boundaries from one dynamical mode to another. A multi-modal planning algorithm is sought to robustly find paths in composite configuration space whilst avoiding the emerging challenges with composite space and handling the uncertainty introduced by the lack of environmental knowledge. A number of researchers tackled this problem. In the following, we provide a categorization and a summary of the methods, advantages and disadvantages of the most relevant state-of-the-art methods.

Locally Optimal Approaches As indicated in the previous paragraph, finding a path in the composite configuration space cannot computationally be found in a reasonable time (orders of magnitude slower than real-time, with no guarantees if no path exists). Only by leveraging simplifications applied to the

composite configuration space can a search be performed, such as considering a heavily simplified probabilistic environment [37], considering a single manipulation action [4], discretization [29] or a heuristic function combined with a time horizon [29]. Such techniques prevent searching in configurations relatively far from the current configuration. Local optimality guarantees can be given, and real-time implementations have been shown.

The most relevant locally optimal approach is presented by Sabbagh Novin et al. She presents an optimal motion planner [29] and applies it to a robot in a hospital environment [23] to later improve upon her work [30]. The optimal motion planner avoids obstacles in the workspace and respects the kinematic and dynamic constraints of a robot arm [29]. Examples of the motion planner are provided using a 3- and 4- Degrees Of Freedom (DOF) planar robot arm. Sampling in the composite configuration space is simplified using discretization (by disjunctive programming [9]) of the composite configuration space and by using a receding horizon. The disjunctive programming concept is applied to convert the continuous problem of path planning into a discrete form. In other words, a continuous path is made equivalent to some points with equal time distances representing the entire path. After discretization, the composite configuration space remains untraceable. Thus a search is performed close to the current configuration by combining a heuristic function with a receding horizon concept. A specially developed heuristic function points *toward* a target configuration. The planner then plans between the current configuration and a point toward the target configuration for a predetermined time horizon. The concept of a receding horizon is used to obtain the optimal path for every time step in the time horizon, but apply only the first term and repeating this process until the end-effector meets the final position.

The optimal motion planner [29] is then converted toward path planning for a nonholonomic mobile robot with a gripper [23]. With the 3-fingered gripper, the robot can grasp legged objects such as chairs or walkers. The targeted workspace is a hospital where the robot is tasked with handing walkers (or other legged objects) to patients to lower the number of falling patients. The variety of legged objects motivates an object model learning module that learns dynamic parameters from experimental data with legged objects. The dynamic parameters are learned using a Bayesian regression model [31]. An MPC controller then tracks the path and compensates for modelling errors. An essential contribution is that the planner can decide to re-grasp one of the object's legs to improve path tracking.

Real-world experiments show the effectiveness of Novin's locally optimal approach [30]. She has presented a manipulation planning framework focused on moving legged objects in which the robot must choose which leg to push or pull. The framework can operate in real-time, and the local optimality has been shown. From the three topics this thesis focuses on, Sabbagh Novin et al. includes learning object dynamics and prehensile manipulation of objects to target positions, missing only the NAMO problem because a path is assumed to be free during object manipulation. Because Novin uses a gripper to manipulate objects, her research falls into the category of prehensile manipulation. Nonprehensile manipulation bears an additional challenge over prehensile manipulation. With prehensile manipulation, a gripper ensured multiple contact points, geometrically locking the object with respect to the gripper. Until the gripper opens, the gripper and gripped object can be considered a unified object. Nonprehensile manipulation, unlike prehensile manipulation, does not have the advantage of locking the object in place, making it more challenging.

Hierarchical Approaches The second class of approaches to finding a path in composite configuration space is classified as hierarchical approaches [11, 19, 31, 38, 40] that can be described as follows. A hierarchical structure generally consists of a high-level and a low-level component. The high-level task planner has an extended time horizon, including several atomic actions and their sequencing. Whilst a low-level controller acts to complete a single action in a single mode of dynamics, e.g. drive toward the object, push object. The high-level planner has a prediction horizon consisting of an action sequence, a long prediction horizon compared to the low-level planner, whose prediction horizon is, at most, a single action.

The most relevant hierarchical approach is presented by Scholz et al. [31]. He presents a planner for the NAMO problem that can handle environments with under-specified object dynamics. The robot's

workspace is split into various regions where the robot can move freely. Such regions can be connected if an object separates two regions and can be manipulated by the robot to connect both regions. The manipulation action is uncertain because objects have constraints that the robot has to learn, e.g. a table has a leg that only rotates but cannot translate. A Markov Decision Process (MDP) is chosen as a graph-based structure, where the nodes represent a free space region and objects separating the regions are edges in the MDP. Finding a solution for the MDP leads to an action sequence consisting of some drive and object manipulation actions to drive the robot toward a target position eventually. The under-specified object dynamics introduce uncertainty in object manipulation. During action execution, object constraints are captured with a physics-based reinforcement learning framework that results in improving manipulation planning when replanning is triggered.

Scholz et al. presented a NAMO planner that makes use of a hierarchical MDP combined with a learning framework, resulting in online learning of the under-specified object dynamics. An implementation on a real robot has shown the method's effectiveness in learning and driving toward a target location. From the three topics this thesis focuses on, Scholz et al. includes learning and the NAMO problem, missing only push manipulation toward target locations. By not including manipulating objects to target positions Scholz et al. can find a global path without running into high dimensional spaces. In other words, by driving only the robot toward a target location, a global path will encounter objects only once. By running into objects only once, manipulating an object does not affect the feasibility of the global path, hence the simplification.

Individually a considerable amount of research is done on these three topics (learning object dynamics [6, 32], NAMO [5, 10, 11, 17, 20, 40], nonprehensile pushing [2, 3, 21, 34, 35, 36]). Combining two topics received little attention from the scientific community, and combining all three topics (to the best of my search) not at all. Table 1.1 presents state-of-the-art literature and which portion of the three topics they include in their research. The most relevant work for local optimal [30] and hierarchical [31] approaches are discussed, both having advantages and disadvantages. Local optimal approaches converge to a local optimal plan. To avoid the curse of dimensionality, simplifications must be used to sample the composite configuration space to be computationally feasible. Such simplifications determine the quality of solutions found. Hierarchical structures generally provide computationally efficient solutions but are hierarchical, meaning the solutions found are the best feasible solutions in the task hierarchy they search. The quality of the solution depends on the hierarchy, which is typically hand-coded and domain-specific [38]. Note that both relevant works focus on prehensile manipulation, whilst this thesis focuses on nonprehensile push manipulation.

Author	Citation	Learns object dynamics	NAMO		Specify object target poses	
			prehesile	nonprehesile	prehesile	nonprehesile
Ellis et al.	[11]	✓	✗	✓	✗	✗
Sabbagh Novin et al.	[30]	✓	✓	✗	✓	✗
Scholz et al.	[31]	✓	✓	✗	✗	✗
Vega-Brown and Roy	[38]	✗	✓	✗	✓	✗
Wang et al.	[40]	✗	✗	✓	✗	✗
Groote	Proposed Framework	✗/✓	✗	✓	✗	✓

Table 1.1: Overview of topics; learning object dynamics, NAMO and specifying target poses in recent literature. This thesis combines the three topics; learning object dynamics, NAMO and nonprehensile pushing.

1.1. Research Question

The following research questions have been selected to investigate the effect of learning on action selection and action planning.

Main research question:

How do learned objects' system models improve global task planning for a robot with nonprehensile push manipulation abilities over time?

The main research question is split into two smaller, more detailed subquestions.

Research subquestion:

1. How to combine learning and planning for push and drive applications?
2. How do learning system models and remembering interactions compare to only learning system models? Furthermore, how does the proposed framework compare against the state-of-the-art?

This thesis's main contribution is combining all three topics. These topics are learning object dynamics, the NAMO problem and nonprehensile push manipulation. The proposed framework combines these three topics with the *hypothesis algorithm*. The algorithm builds a graph-based structure with nodes and edges, named the *hypothesis graph*. Planning directly in the composite configuration space is avoided. The hypothesis algorithm plans only in a single mode of dynamics and searches for a global path with a technique known as a backward search [19]. Learned object dynamics are stored in a knowledge base called the *knowledge graph*. The halgorithm, hgraph and kgraph are introduced in Chapter 3.

1.2. Problem Description

To help answer the research questions, tests are performed in a robot environment. A simple environment is desired because that simplifies testing, yet the robot environment should represent many real-world environments in which robots operate. Thus a 3-dimensional environment is selected. The environment consists of a flat ground plane since many mobile robots operate in a workspace with a flat floor, such as a supermarket, warehouse or distribution center. An environment with a flat floor and a flat robot can be treated as a 2-dimensional problem because the robot and objects can only change position over x

and y axis (xy plane parallel to the ground plane) and rotate around the z axis (perpendicular to the ground plane). A flat robot is selected because it has a low center of gravity, which lowers the chance of tipping over.

Let us start with defining the environment. Let the tuple $\langle \text{Origin}, \text{Ground Plane}, Obj, Eq \rangle$ fully define a robot environment where:

- Origin Static point in the environment with a x -, y - and z -axis. Any point in the environment has a linear and an angular position and velocity with respect to the origin
- Ground Plane A flat plane parallel with the Origin's x - and y - axis. Objects cannot pass through the ground plane and meet sliding friction when sliding over the ground plane.
- Obj A set of objects, $Obj = (ob_1, ob_2, ob_3, \dots, ob_i)$ with $i \geq 1$, an object is a 3-dimensional body with shape, can be unmovable or movable. In the latter case, the mass is uniformly distributed. The robot itself is considered an object, an environment thus contains one or more objects. Examples of objects are given in Figure 1.2.
- Eq A set of motion equations describing the behaviour of objects.

A configuration consists of the linear position of an object's center of mass with respect to the environment's origin and the angular position of an object's orientation with respect to the environment's origin.

Formally, a **configuration**, $c_{id}(k)$ is a tuple of $\langle pos_x(k), pos_y(k), pos_\theta(k) \rangle$ where $pos_x, pos_y \in \mathbb{R}$, $pos_\theta \in [0, 2\pi)$. k indicates the time step and can be dropped to simplify the notation, id is short for identifier and indicates the object to which this configuration belongs.

1.2.1. Task Specification

To answer the research questions, a number of tasks are designed, which are defined as a subset of all objects with an associated target configurations.

$$\text{task} = \langle Obj_{task}, C_{targets} \rangle$$

where $Obj_{task} \subseteq Obj$, $C_{target} = (c_1, c_2, c_3, \dots, c_k)$ and $k > 0$.

A task is completed when the robot manages to push every object to its target configuration within a specified error margin.

1.2.2. Assumptions

To simplify the pushing and learning problem, several assumptions are taken, which are listed below.

Closed-World: Objects are manipulated, directly or indirectly only by the robot. Objects cannot be manipulated by influences from outside the environment.

Perfect Object Sensor: the robot has full access to the poses and geometry of all objects in the environment at all times.

Tasks are Commutative: Tasks consist of multiple objects with specified target positions. The order in which objects are pushed toward their target position is commutative.

3-dimensional robot environment can be represented as 2-dimensional environment All objects in the environment can be projected onto the ground plane.

The assumptions taken serve to simplify the problem of task completion. Note that in Section 5.1 insight is given to remove all assumptions. By removing assumptions completing tasks becomes a harder problem, but a more realistic problem closer to real-world applications.

Assumptions might have certain implications, which are listed below. The **closed-world assumption** implies that objects that stand still and did not interact with the robot remain at the same position. Completed subtasks are therefore assumed to be completed for all times after completion time.

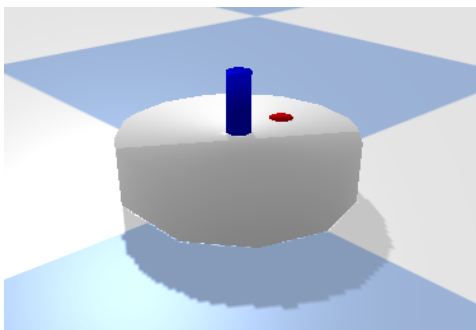
The **perfect object sensor assumption** simplifies a sensor setup, it prevents Lidar-, camera setups and tracking setups with aruco or other motion capture markers. The existence of a single perfect measurement wipes away the need to combine measurements from multiple sources with sensor fusion algorithms, such as Kalman filtering [39].

Certain tasks are only feasible if performed in a certain order (e.g. the Tower of Hanoi). The **tasks are commutative assumption** allows focusing only on a single subtask since it does not affect the completion or feasibility of other subtasks.

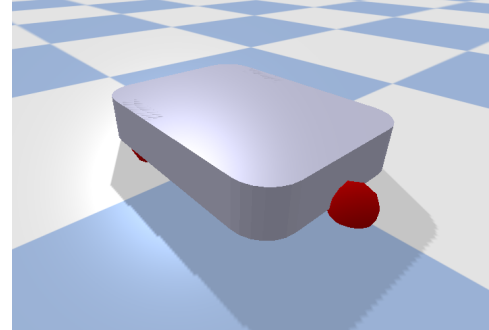
The **3-dimensional world can be represented as 2-dimensional** ensures that the objects in the environment can be projected onto the ground plane. Additionally it ensures that objects do not tip over. In practice, objects will not be higher than the minimum width of the object. This experimental strategy seemed sufficient whilst running experiments but does not guarantee that objects cannot tip over.

1.2.3. An Example of Robots and Objects

To get a sense of what the robots and the objects look like, see the two robots that are used during testing in Figure 1.1. And among many different objects, two example objects are displayed in Figure 1.2.



(a) The holonomic point robot with velocity input in x and in y direction



(b) The nonholonomic boxer robot, the input is forward and rotational velocity

Figure 1.1: Two robots in the simulation environment

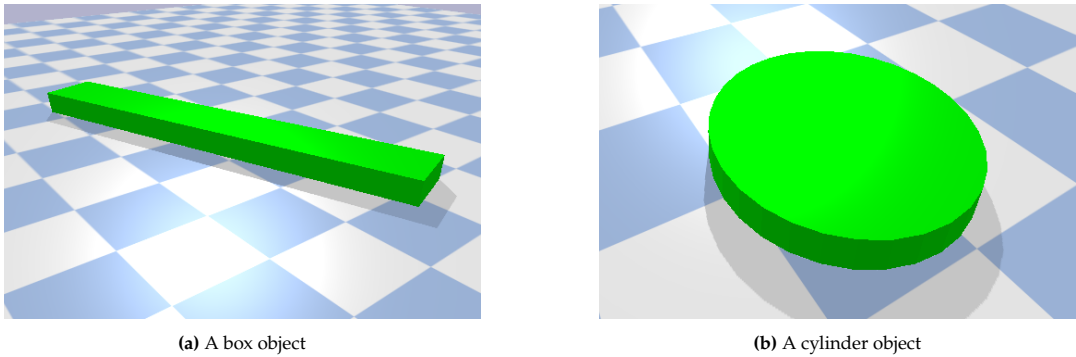


Figure 1.2: Two objects in the robot environment

For complete environments with accompanying tasks, see Chapter 4.

1.3. Report Structure

The proposed framework heavily relies on a number of methods and functions. These methods and functions are conveniently grouped in Chapter 2. Then the proposed framework is presented and discussed in Chapter 3. Testing the proposed framework is presented in Chapter 4. The last chapter draws conclusions on tests and answering the research questions.

2

Required Background

This chapter presents the components that the proposed framework relies upon, the required background. These components are: system identification, control methods, planning and finally fault detection. System identification is responsible for converting Input-Output (IO) data into a system model as described in Section 2.1. In the scope of this thesis a system model is required by control methods in order to create stable control and to track a reference signal. Control methods are presented in Section 2.2. Path planning is a core component of the proposed framework and is responsible for finding a path in configuration space. Such a path acts as reference signal for the controller and planning detects objects that are blocking the path, and must be removed first. The planning component is split into path estimation in Section 2.3.1, motion planning in Section 2.3.2 and manipulation planning in Section 2.3.3. Lastly fault detection halts persisting faulty behavior and will be elaborated upon in Section 2.4.

2.1. System Identification

Understanding the world by a robot is captured by models, *system models* that estimate the behavior of real-world systems. For example what trajectory does an object take after receiving a push? The trajectory is dependent on the properties of the object (e.g. mass, geometry), and interaction with its surroundings (e.g sliding friction). These properties and interactions are captured by a system model. Just as applicable constraints that are captured by a system model, see both robots in Figure 1.1, the holonomic point robot in Figure 1.1a can drive without constraints, and the boxer robot in Figure 1.1b can drive forward, backwards and can rotate. A system model for robot driving for the boxer robot should thus capture that it is not able to drive directly sideways.

Robots encounter a wide variety of objects because every object can be different in type, weight and dimensions. System identification methods are required to capture the variety of objects that the robot can encounter.

Visualise test push sequence to collect IO data, once with the robot to generate a system model for drive applications

Visualise test push sequence to collect IO data, once with the robot and object to generate a system model for push applications

Note that theoretically a system identification module is included in the proposed robot framework. For the implementation the system identification module is left out for time related reasons. Firstly creating the implementation module itself takes time. Secondly, collecting enough IO data to generate a system model is timewise very costly. Thus by using several hard-coded system models instead of implementing a system identification module time is saved. The replacement moves focus from “which system identification method yields a system model that most accurately describes a dynamic model?” to “which system model in the set of available models most accurately describes a dynamic model?”.

Implementing a system identification module is moved to the future work section. To keep the

option of implementing the system identification module open, the system identification module is kept in the proposed robot framework.

2.2. Control Methods

This section elaborates why control is required and which control methods are best suitable for various control applications. During this thesis, the effect of the robot interacting with objects is captured by system models. In addition to predicting output with system models, control methods leverage the prediction that system models provide to perform actions, in this thesis drive and push actions. A requirement for a controller is that it should yield a stable closed-loop control because that guarantees converging toward a set point. Controllers are later, in the proposed framework selected for yielding desired metrics such as a low prediction error, low tracking error and low final placement error, such metrics are grouped in Section 2.4. The two control methods that are used during testing are discussed below.

Model Predictive Control The basic concept of MPC is to use a dynamic model to forecast system behaviour and optimise the forecast to produce the best decision for the control move at the current time. Models are therefore central to every form of MPC [26]. The best feasible input is found every time step by optimising the objective function whilst respecting constraints. Tuning is accomplished by modifying the weight matrices in the objective function, or by modifying the constraint set. Solving an objective function to find the best feasible input generally yields robust control. System models for driving the robot can be estimated with Linear Time-Invariant (LTI) models without compromising on model accuracy making MPC controllers a suitable candidate for driving actions. A more elaborate description of MPC control can be found in Appendix B.

Model Predictive Path Integral Control The core idea is from the current state of the system with the use of a system model and randomly sampled inputs to simulate in the future several “rollouts” for a specific time horizon, [22]. These rollouts indicate the future states of the system if the randomly sampled inputs would be applied to the system, the future states can be evaluated by a cost function which penalized undesired states and rewards desired future states. A weighted sum over all rollouts determines the input which will be applied to the system. The main advantage MPPI has over MPC control is that it is better suited for nonlinear system models. Whilst drive applications can be accurately estimated by linear models, push applications are harder to estimate with a linear model. Thus MPPI is selected mainly for push applications. A more elaborate description of MPPI control can be found in Appendix B.

The properties of MPC suggest that it is best suitable for drive actions because of easy tuning and robustness. MPPI control is compatible with nonlinear system models, making it best suitable for push actions. It is worth mentioning that the goal of this thesis is not to find the best optimal controller. The goal is to gradually over time choose control methods in combination with system models that result in better performance, the performance is measured with various metrics to which Section 3.2.3 is dedicated.

2.3. Planning

This section explains planning for a single drive or push action as *local planning*. Local planning consists of 2 steps, firstly, path estimation, and secondly, motion or manipulation planning. The path estimator can detect non-existent paths and concludes such paths as unfeasible. For the remainder of actions, motion or manipulation planning is responsible for finding a path from starting point to a target point in configuration space. The planner has to account for multiple subspaces in configuration space (free, obstacle, movable and unknown space). An existing motion planner [5] extends to incorporate movable and unknown spaces next to the conventional free and obstacle spaces. The modification incentivizes the planner to find a path in free space but can pass through unknown or movable space as a last resort.

The robot should first remove the blocking objects if a planned path crosses an unknown or movable subspace.

2.3.1. Estimating Path Existence

In this subsection, motivation and explanation for estimating path existence are presented. We can describe the path estimation algorithm as *The idea is to discretize the configuration space. The emerging cells act as nodes in the graph, cells connect through edges to nearby cells. Graph-based planners start from the cell containing the starting configuration and search for the cell containing the target configuration while avoiding cells in obstacle space.*

If the path estimator concludes the existence of a path planning problem, then it is validated that it is geometrically possible for an object to go from start to target configuration in small successive steps without colliding with an unmoving obstacle. The check prevents the planner from attempting a search for a start and target configuration for a problem that is unfeasible due to not being detected by the path estimator because it does not check for nonholonomic constraints. By neglecting nonholonomic constraints, the path estimator is magnitudes faster than the planner; the planner is responsible for checking the nonholonomic constraints.

Discretizing the Configuration Space For general geometric shapes, a configuration space can be constructed and discretized. During this thesis, configuration space was implemented for cylinders and rectangular prisms. First, the configuration space for a cylindrical-shaped object in a 3-dimensional environment is presented. That configuration space for cylindrical objects is defined as a (x, y) -plane, and the z -axis is omitted. During the projection from a 3-dimensional environment to a 2-dimensional plane, cylinders (flat side facing down) become circles, and rectangular prisms become rectangles. The definition of configuration space is presented below for a circular object, such as the point robot, without loss of generality.

A grid of cells represents configuration space. Let s_{cell} be the width and height of a square cell. Let x_{grid} be the vertical (north to south) length and let y_{grid} be the horizontal length (west to east) of the configuration space, point $(0, 0)$ is at the center of the grid.

The configuration space for a circular object is defined as:

$$\text{C-space}^{\text{circle}} = \begin{bmatrix} c_{(0,0)} & c_{(0,1)} & \dots & c_{(0,j_{\max})} \\ c_{(1,0)} & c_{(1,1)} & \dots & c_{(1,j_{\max})} \\ \vdots & \vdots & \ddots & \vdots \\ c_{(i_{\max},0)} & c_{(i_{\max},1)} & \dots & c_{(i_{\max},j_{\max})} \end{bmatrix}$$

$$\text{with } 0 \leq i \leq i_{\max} = \frac{x_{grid}}{s_{cell}}, \quad 0 \leq j < j_{\max} = \frac{y_{grid}}{s_{cell}}$$

Where $c_{(i,j)}$ in matrix C-space represents to which subspace the cell at indices (i, j) belongs. The four subspaces considered in this thesis are free-, obstacle-, movable- and unknown space indicated with the integers 0, 1, 2 and 3, respectively. Multiple subspaces can reside in a single cell; by default, a cell represents free space. The subspaces are ordered from least to most important: free, movable, unknown, and obstacle space. A cell displays the subspace with the highest order of importance that resides in the cell. Thus a cell that contains part unknown and part obstacle space will evaluate as obstacle space since obstacle space has a higher order of importance than the unknown space.

A mapping function $f_{chart_to_idx}(i, j)$ maps the Cartesian (x, y) coordinates to their associated (i, j) indices:

$$f_{chart_to_idx}(i, j) : \mathbb{R}^2 \mapsto \mathbb{Z}_{\geq 0}^2$$

Defined for:

$$x = \{x_{grid} \in \mathbb{R} : -\frac{x_{grid}}{2} \leq x \leq \frac{x_{grid}}{2}\}, \quad y = \{y_{grid} \in \mathbb{R} : -\frac{y_{grid}}{2} \leq y \leq \frac{y_{grid}}{2}\}$$

A mapping function $f_{idx_to_chart}(i, j)$ maps the indices (i, j) to their associated charthesian (x, y) coordinates:

$$f_{chart_to_idx}(i, j) : \mathbb{Z}_{\geq 0}^2 \mapsto \mathbb{R}^2$$

Defined for:

$$i = \{\frac{x_{grid}}{s_{cell}} \in \mathbb{Z}_{\geq 0} : 0 \leq i \leq \frac{x_{grid}}{s_{cell}}\}, \quad j = \{\frac{y_{grid}}{s_{cell}} \in \mathbb{Z}_{\geq 0} : 0 \leq j \leq \frac{y_{grid}}{s_{cell}}\}$$

For rectangular objects, the orientation of the object becomes important because the orientation, together with the (x, y) coordinates, determines which subspace the object resides. The dimension for rectangular objects is thus 3, whilst circular objects have a 2-dimensional configuration space.

The configuration space for a rectangular object is defined as:

$$\text{C-space}^{rectangle} = \begin{bmatrix} c_{(0,0,0)} & c_{(0,1,0)} & \dots & c_{(0,j_{max},0)} \\ c_{(1,0,0)} & c_{(1,1,0)} & \dots & c_{(1,j_{max},0)} \\ \vdots & \vdots & \ddots & \vdots \\ c_{(i_{max},0,0)} & c_{(i_{max},1,0)} & \dots & c_{(i_{max},j_{max},0)} \end{bmatrix} \begin{bmatrix} ,1)) & c_{(i_{max},1,1))} & \dots & c_{(i_{max},j_{max},1))} \\ \vdots & \vdots & \ddots & \vdots \\ c_{(0,0,1)} & c_{(0,1,1)} & \dots & c_{(0,j_{max},1)} \\ c_{(1,0,1)} & c_{(1,1,1)} & \dots & c_{(1,j_{max},1)} \\ \vdots & \vdots & \ddots & \vdots \\ c_{(i_{max},0,1)} & c_{(i_{max},1,1)} & \dots & c_{(i_{max},j_{max},1)} \end{bmatrix} \begin{bmatrix} c_{(0,0,k_{max})} & c_{(0,1,k_{max})} & \dots & c_{(0,j_{max},k_{max}))} \\ c_{(1,0,k_{max}))} & c_{(1,1,k_{max}))} & \dots & c_{(1,j_{max},k_{max}))} \\ \vdots & \vdots & \ddots & \vdots \\ c_{(i_{max},0,k_{max}))} & c_{(i_{max},1,k_{max}))} & \dots & c_{(i_{max},j_{max},k_{max}))} \end{bmatrix}$$

$$\text{with } 0 \leq i \leq i_{max} = \frac{x_{grid}}{s_{cell}}, \quad 0 \leq j \leq j_{max} = \frac{y_{grid}}{s_{cell}}, \quad k \in \mathbb{Z}_{\geq 0}.$$

Similar to $f_{chart_to_idx}(x, y)$ and $f_{idx_to_chart}(i, j)$ the mapping functions $chart_to_idx(x, y, \theta)$ and $f_{idx_to_pose}(i, j, k)$ exist and map between the (x, y, θ) pose and the (i, j, k) indices.

An example configuration space for the point robot is presented below.

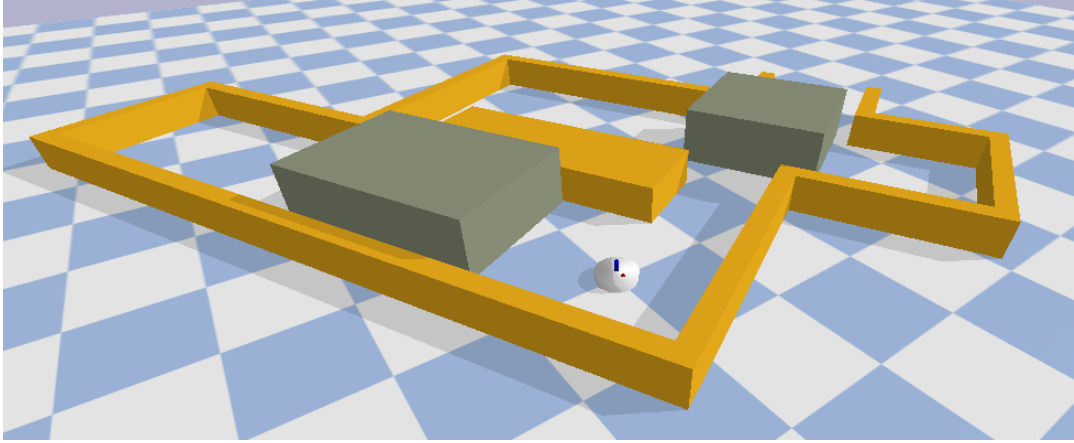


Figure 2.1: Environment with the point robot, unmovable yellow walls and movable brown boxes. The robot classifies all objects as unknown since it is unaware of the objects' classes.

The point robot has a cylindrical shape; thus, a 2-dimensional configuration space is created and can be seen in Figure 2.2.

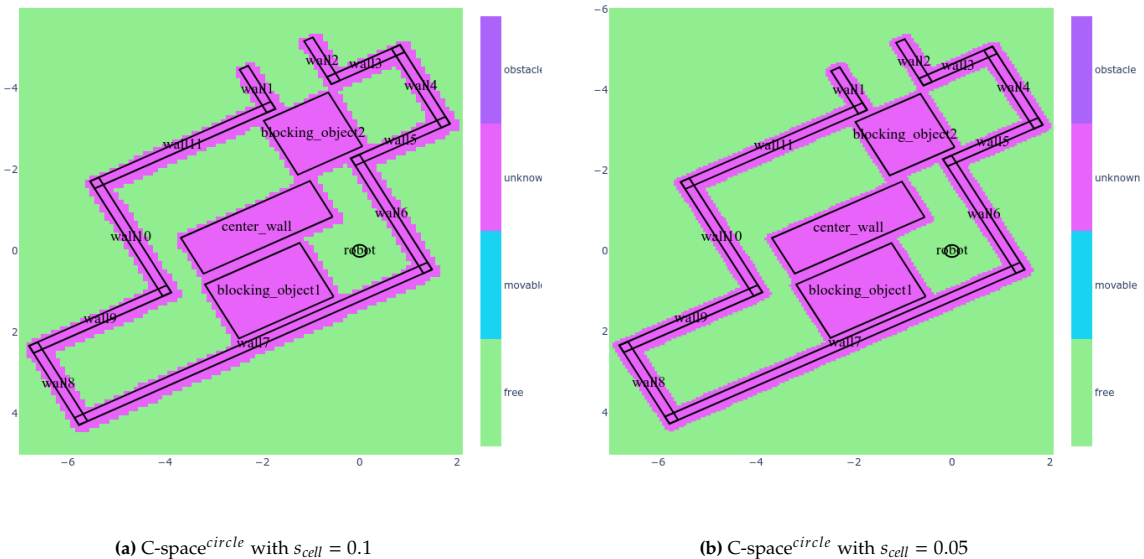


Figure 2.2: The configuration space for the point robot with different cell sizes. The robot environment corresponds to the environment presented in Figure 2.1.

The resolution of the configuration space at Figure 2.2b is higher compared to Figure 2.2a because of a smaller grid size. A high resolution is better at detecting paths through small corridors and tight corners, but it comes at the cost of a more extended creation and search time.

Path Existence Algorithm In the context of this thesis, we can describe path existence as *For an object's configuration space, there exists a list of neighbouring cells from starting to target configuration that does not lie in obstacle space.*

A path in configuration space is detected using the implemented $f_{shortest_path}(c_{start}, c_{target}, detect_blocking_objects)$ function. This function returns the shortest path from the c_{start} to the c_{target} . $detect_blocking_objects$ is a boolean flag that if *True* returns a list blocking objects classified as movable or unknown. If no path is found, the $f_{shortest_path}$ function raises an error.

The *shortest_path* function uses the Dijkstra algorithm [8] on the discretizing configuration space to find a shortest path. This path can be converted to provide an initial number of path planner samples, also referred to as a “warm start”.

Unfeasible solutions and an undecidable problem The path estimation algorithm does not take system constraints into account. Thus, the path estimation algorithm can find a list of neighbouring cells from the start to the target configuration and conclude that a path exists. In reality, this path is unfeasible. An example is driving the boxer robot displayed in Figure 1.1b through a narrow, sharp corner. Whilst geometrically, the robot would fit through the corner, the nonholonomic constraints of the robot prevent it from steering through such a tight corner. It is for the motion or manipulation planner to detect that the path is unfeasible.

The path estimator suffers from another drawback, finding proof that there exists a path that is undecidable [42]. This is due to the chosen cell size during discretizing the configuration space. An example is a corridor having the same width as the robot. The robot fits exactly through this corridor. Detecting such a path requires many neighbouring cells that lie exactly in the centre line of the corridor. Only with a cell size going to zero and the number of cells going to infinity such a path is guaranteed to be detected. Path non-existence, on the other hand, is easier to prove because the path estimation algorithm provides an upper bound on existing paths and a lower bound on non-existing paths [42].

The path existence algorithm can detect non-existence paths. Thus checking path existence before motion or manipulation planning filters out several non-existent paths saving time and resources. Even if, in exceptional cases, the path estimation algorithm can yield unfeasible paths and can fail to detect existing paths. Checking path existence before path planning filters some non-existent paths and is additionally motivated by two reasons. First, path estimation is orders of magnitude faster compared to motion or manipulation planning. Secondly, the path estimation algorithm can provide a number of initial samples to the motion or manipulation planner that can act as a “warm start”.

A path is a list of successive configurations beginning with the start and ending with the target configuration. During planning, constraints are respected by checking the reachability of the configurations added to the path with a system model.

2.3.2. Motion Planning

Controllers discussed in Section 2.2 can track a path from start to target, given that all necessary ingredients are provided. Providing a path is the planners’ responsibility; planners seek inside the configuration space for a path from the start to the target configuration. A practical example of such a path is a list of successive points in configurations space. The first point is the start configuration, and the last is the target configuration. How far the successive points can lie apart is a tuning parameter of the planner. Seeking a path from start to target inside a configuration space whilst avoiding obstacles for the robot to track is referred to as *motion planning*. Finding a path between the start and target configuration for pushing applications whilst avoiding collisions is referred to as *manipulation planning*. This and the upcoming subsection present two new sample-based planners (one for drive and one for push applications); they are based upon an existing double tree optimised Rapidly-exploring Random Tree (RRT*) planner [5]. The existing planner plans in free and obstacle space; a modification extends the planner to incorporate movable and unknown space. First, this section presents the new motion planning algorithm, and the next section, Section 2.3.3 dedicates itself to manipulation planning. The new planning algorithms are sample-based, which can be described as.

“The main idea is to avoid the explicit construction of the object space and instead conduct a search that probes the configuration space with a sampling scheme. This probing is enabled by a collision detection module, which the motion planning algorithm considers a “black box.” [20]”

Generally, the configuration space consists of 2 subspaces, free- and obstacle space. The configuration space in this thesis consists of 4 subspaces: free, obstacle, unknown and movable space. A dedicated path planning algorithm has been developed to solve planning problems for such a configuration

space with four subspaces. The newly developed path planner extends the existing double tree RRT* algorithm [5]. The motion planner consists of the following.

$$V_{MP} : \text{A set of nodes}$$

$$E_{MP} : \text{A set of edges}$$

$$P : \text{A set of paths}$$

The start connectivity tree consists of the nodes connected by edges containing the starting node, and vice versa for the target connectivity tree containing the target node. The algorithm grows the two *connectivity trees* by randomly sampling configurations and adding them to the start or target connectivity tree. The algorithm explores configuration space by growing these connectivity trees. When the start connectivity tree is close enough (inside the search size of a newly added sample) to the target connectivity tree, a path from start to target is found. The goal of the motion planner is to find a path between the start and target configuration that results in the lowest totalPathCost, defined as:

$$\text{TotalPathCost} = \text{PathCost} + \text{MovableSpaceCost} + \text{UnknownSpaceCost}$$

The PathCost corresponds to the sum of euclidean distances between the successive configurations in the path. The MovableSpaceCost and UnknownSpaceCost correspond to a fixed addition cost for a configuration in the path that crosses through movable or unknown subspace, respectively. Crossing through is defined as one or more nodes in the path lying in that subspace. If a path does not contain a node in movable space, MovableSpaceCost will be 0, equivalent to unknown space and UnknownSpaceCost. Optimizing the path for the lowest cost incentivizes the motion planning algorithm to find a path around unknown or movable objects. Newly sampled configurations are added structurally, guaranteeing an optimal path is found with infinite sampling [5]. Where optimality is defined as the path with the lowest possible cost.

Tuning Parameters The algorithm has four tuning parameters that can be tweaked; first, the *step size*, the maximal normalized distance between connected samples in the connectivity trees, see Figure 2.3c for a visual example. Choosing a high step size will increase search speed because the connectivity trees grow faster. A higher step size comes at the cost of smoothness; the resulting path will be bumpier with sharper corners. Additionally, the path has an increased chance of collision with obstacles because, for two connected configurations in a path, the individual configurations can both lie in free space. The space between configurations is not checked, and an obstacle could be in between the configurations, especially when cutting corners around obstacles. The second tuning parameter is the *search size*, which is a subspace around the newly sampled sample (see, Figure 2.3d). In this subspace, a parent node is sought, and rewiring occurs. A parent node connects a new node with an edge to a connectivity tree. After connecting the new node to its parent node, rewiring occurs, changing the parent node by removing and adding an edge. If that results in a lower cost for that node, rewiring can be visually seen in Figure 2.3e. Increasing the search size improves the choice of the parent node and improves cost due to rewiring, but it also exponentially increases computation time. The third and fourth tuning parameters are the fixed costs for crossing through movable or unknown space, Figure 2.5 clearly shows the effect of varying such costs.

The Pseudocode of the proposed algorithm is provided in Algorithm 1. The functions used are elaborated upon in the following Table 2.1.

x :	A node representing a point in configuration space
x_{init} :	Creates a start and target node
$NotReachStop$:	True if the stopping criteria are not reached
$Sample_{random}$:	Creates a random sample in free-, movable- or unknown space
$Nearest(x, V)$:	Returns the nearest nodes from x in V
$NearestSet(x, V)$:	Returns set of nearest nodes from x in V
$Project(x, x')$:	Project x toward x'
$CollisionCheck(x)$:	Returns true if x is in free-, movable- or unknown space
$ObjectCost(x', x)$:	Returns a fixed additional cost if x enters movable- or unknown space from x' , otherwise returns 0
$Distance(x, x')$:	Returns the distance between sample x and x'
$CostToInit(x)$:	Find the total cost from x to the initial node
$ReachabilityCheck(x, x')$:	Return true if a system model with initial state x can reach state x' for a range of allowed input; otherwise, return false.
$InSameTree(x, x')$:	Returns true if both x and x' are in the same tree, otherwise return false

Table 2.1: Functions used by the Algorithm 1

Notice that in Algorithm 1, the coloured sections correspond to the surrounding coloured border in the subfigures of Figure 2.3.

Algorithm 1 Pseudocode for modified double tree RRT* algorithm

```

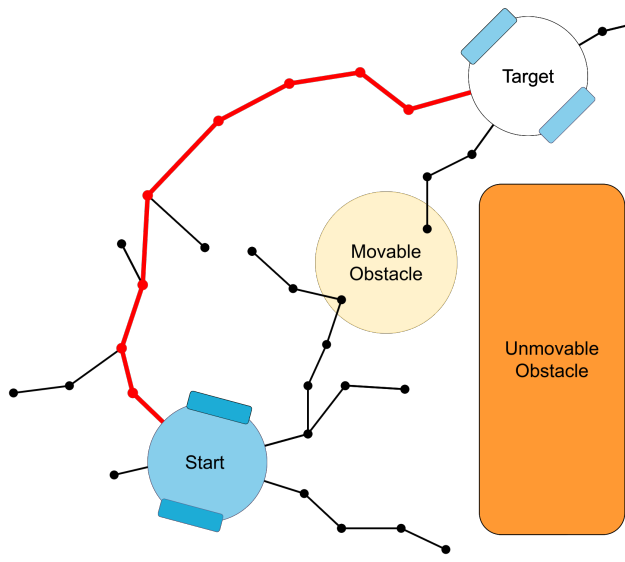
1:  $V_{MP} \leftarrow x_{init}$ 
2: while NotReachStop do
3:    $Cost_{min} \leftarrow +\infty$                                 ▷ Create, check and project a new random sample
4:    $v_{rand} \leftarrow Sample_{random}$ 
5:    $v_{nearest} \leftarrow Nearest(v_{rand}, V_{MP})$ 
6:    $v_{temp} \leftarrow Project(v_{rand}, v_{nearest})$ 
7:   if CollisionCheck( $v_{temp}$ ) then
8:      $v_{new} = v_{temp}$ 
9:   else
10:    Continue
11:   end if
12:    $X_{near} \leftarrow NearestSet(v_{new}, V_{MP})$                 ▷ Find and connect new node to parent node
13:   for  $v_{near} \in X_{near}$  do
14:      $Cost_{temp} \leftarrow CostFromInit(v_{near}) + Distance(v_{near}, v_{new}) + ObjectCost(v_{near}, v_{new})$ 
15:     if  $Cost_{temp} < Cost_{min}$  then
16:       if ReachabilityCheck( $v_{new}, v_{near}$ ) then
17:          $Cost_{min} \leftarrow v_{temp}$ 
18:          $v_{minCost} \leftarrow v_{near}$ 
19:       end if
20:     end if
21:   end for
22:   if  $Cost_{min} == \infty$  then
23:     Continue
24:   else
25:      $V_{MP}.add(v_{new})$ 
26:      $E.add(v_{minCost}, v_{new})$ 
27:   end if
28:    $Cost_{path} \leftarrow +\infty$                                 ▷ Check if the newly added node can lower cost for nearby nodes
29:   for  $v_{near} \in X_{near}$  do
30:     if InSameTree( $v_{near}, v_{new}$ ) then
31:        $Cost_{temp} \leftarrow CostFromInit(v_{new}) + distance(v_{new}, v_{near}) + ObjectCost(v_{new}, v_{near})$ 
32:       if  $Cost_{temp} < CostFromInit(v_{near})$  then
33:         if ReachabilityCheck( $v_{new}, v_{near}$ ) then
34:            $E.rewire(v_{near}, v_{new})$ 
35:         end if
36:       end if
37:     else                                              ▷ Add lowest cost path to the list of paths
38:        $Cost_{temp} \leftarrow CostFromInit(v_{new}) + distance(v_{new}, v_{near})$ 
39:        $+CostFromInit(v_{near}) + ObjectCost(v_{new}, v_{near})$ 
40:       if  $Cost_{temp} < Cost_{path}$  then
41:         if ReachabilityCheck( $v_{new}, v_{near}$ ) then
42:            $Cost_{pathMin} \leftarrow v_{temp}$ 
43:            $v_{pathMin} \leftarrow v_{near}$ 
44:         end if
45:       end if
46:     end if
47:     if  $Cost_{pathMin} == \infty$  then
48:       Continue
49:     else
50:        $P.addPath(v_{new}, v_{pathMin}, Cost_{pathMin})$ 
51:     end if
52:   end for
end while

```

An example of the proposed algorithm is provided; see Figure 2.3. In this example, one sample is added to the starting connectivity tree. Adding this sample involves many steps: generating a new random sample, projecting the sample to the nearest node, rewiring nearby samples and connecting the start to the target tree.

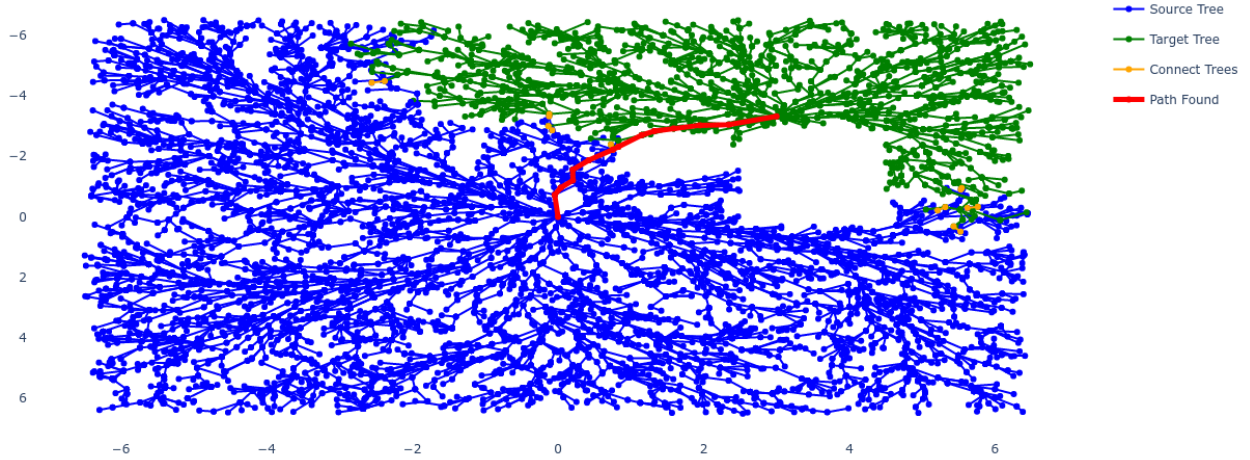


Figure 2.3: Visualization of the Double tree RRT* motion planner that adds a single sample to the connectivity graph. The colour of the box surrounding subfigures corresponds to the coloured sections in Algorithm 1. 3-dimensional configuration space displayed as 2-dimensional configuration space (x and y are visible, θ is not visible).



(a) Motion planner found a path found marked in red.

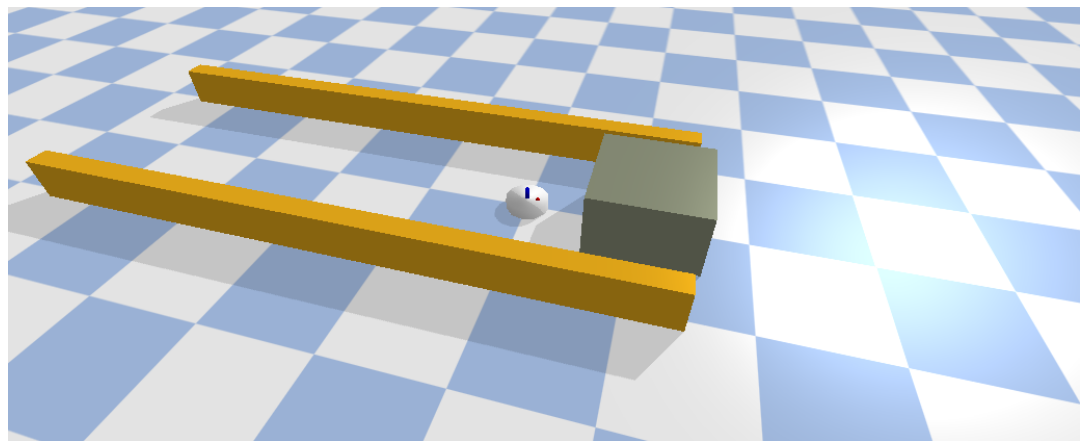
Connectivity Trees



(b) A visualization of the implemented RRT* algorithm when the stopping criteria was reached.

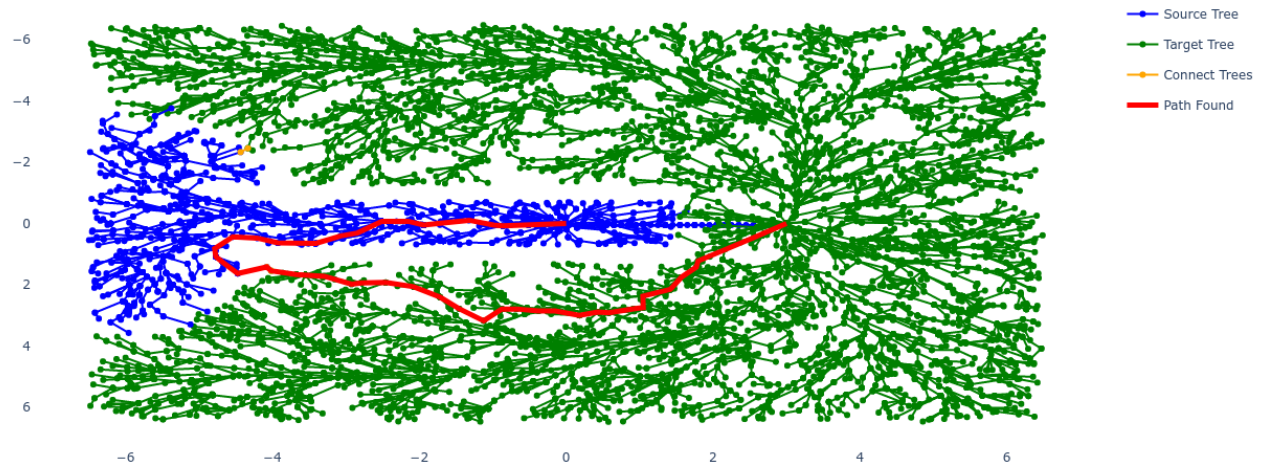
Figure 2.4: Comparing schematic example to a visualization of the real algorithm.

The added fixed cost for a path crossing through a movable or unknown object motivates the motion planner to find the shortest path around objects but prefers moving an object over making a large detour. Tuning the additional fixed cost for a path crossing through movable or unknown space balances the robot's decision between how long of a detour the robot is willing to drive, compared to pushing an object to free the path. Removing an unknown object bears more uncertainty than a movable object, which is why the additional cost to remove an unknown object is higher than that of a movable object.



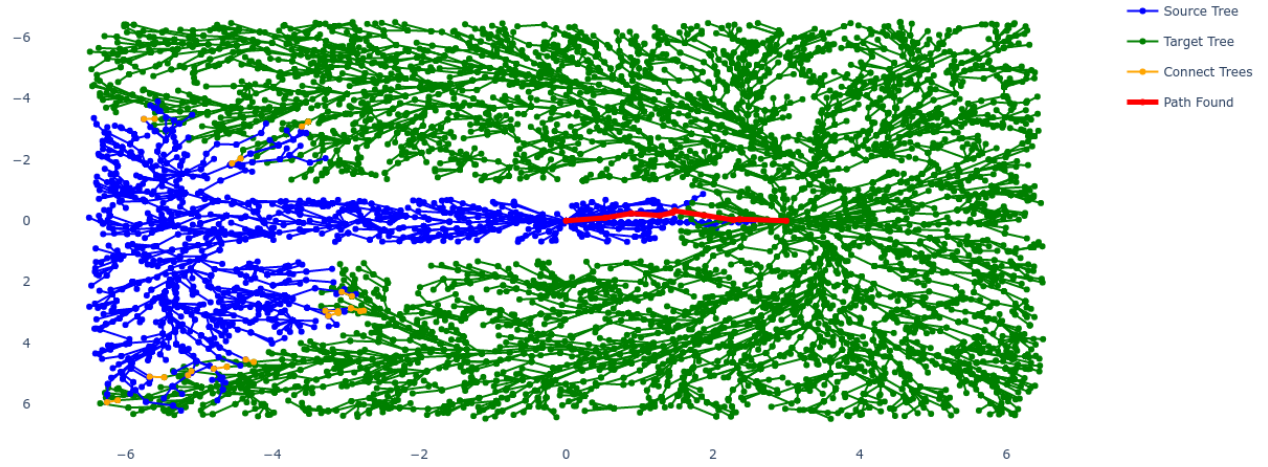
(a) Robot environment with the point robot, two yellow unmovable walls and an unknown brown box.

Connectivity Trees



(b) planned path around the brown box and yellow obstacles, with unknownSpaceCost = 2.

Connectivity Trees



(c) planned path going through the brown box, unknownSpaceCost = 0.5.

Figure 2.5: The robot tasked with driving toward the other side of the brown box.

The proposed motion planning algorithm searches the configuration space from the start to target connectivity trees. Exploring faster than the single tree RRT* algorithm because two trees grow and explore faster than a single tree. The proposed algorithm rewrites nodes, lowering the cost for existing paths and converting to the optimal lowest-cost path with infinite sampling. System constraints are ensured by the *ReachabilityCheck* that validates if a node is reachable from another node using system models.

The proposed algorithm yields feasible paths (according to the system model used to check reachability) that respect the system constraints. The algorithm prevents planning a path through blocking objects except when no other option is available or a large detour can be prevented. There are no performance tests taken on the modified motion planner other than visual inspection. For performance tests and comparison with equivalent sample-based state-of-the-art motion planners, see [5]. Now that motion planning is discussed for drive actions, manipulation will be discussed for push actions.

2.3.3. Manipulation Planning

With a push, two objects are primarily involved, the pushed object and the robot. Generally, and in this thesis, the pushed object's configuration is more important than the robot's configuration. The robot is only a means to push the object toward the target configuration. At which final configuration the robot itself ends up is of lesser importance. As long as during the push, the robot does not collide with objects other than the pushed object, and constraints on the robot must be respected.

To plan a path that respects the constraints, the robot's configuration is generated for every newly added sample in the manipulation planning algorithm. The *ReachabilityCheck()* (see Table 2.1 and line 33 in Algorithm 1) generates the robot configuration to validate if a new sample is reachable from an existing sample. This additional configuration is stored to create only feasible paths that respect the applied constraints. When the stopping criteria are reached and the shortest path is found, the generated robot configurations are discarded. Figure 2.6 displays a visual example of the procedure.

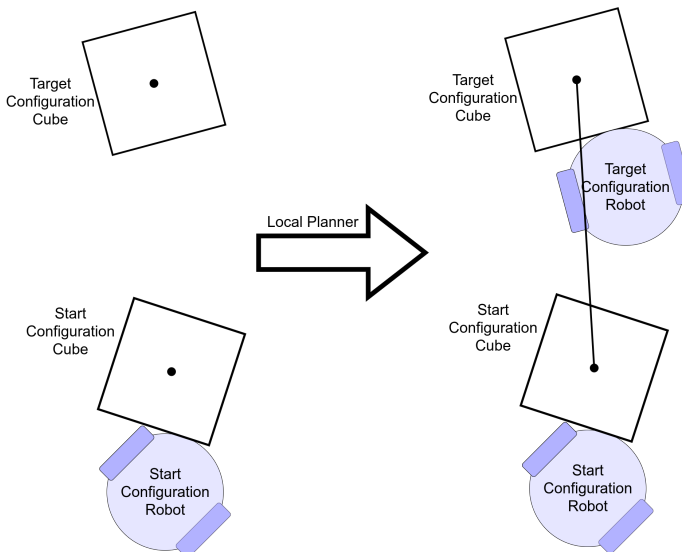


Figure 2.6: Generating a new robot configuration whilst adding a sample to the connectivity tree during manipulation planning.

2.4. Monitoring Metrics

In the next chapter, the proposed framework is discussed, for this section, it is important to know that the proposed framework contains the halgorithm which is responsible for finding action sequences, motion/manipulation planning, and execution of drive and push actions. During the execution time of a drive or push action, the hypothesis algorithm is unable to perform any other action. This blocking behavior has some implications, mainly a controller can steer the system to a state from which it cannot

independently reach the target state, as a result, it will never halt. For example, a controller tries to drive the robot toward a target state but there is an unmovable obstacle in the way. Another example is the controller is closed-loop unstable and never reaches its target state. Both examples do not occur in well defined simulation environments, because of the *closed-world assumption* defined in Section 1.2.2. In the real world, an unexpected blocking obstacle or unstable controller is more likely to occur.

Detecting controller faults is a large robotic topic [16], properly implementing a fault detection and diagnosis module is out of the scope of this thesis. Instead, two simple metrics will be monitored during execution. The first monitoring metric is Prediction Error (PE), the second monitoring metric is Tracking Error (TE). Definitions of the monitoring metrics are summarised in Table 2.2, it also provides insight in which monitoring metric would catch what faulty behavior. The PE and TE are defined as:

$$\epsilon^{pred}(k) := \|\hat{c}(k|k-1) - c(k)\|$$

Where $\hat{c}(k|k-1)$ is a prediction of the configuration and $c(k)$ is the actual configuration.

The Prediction Error can be described as:

Every time step a prediction one step into the future is made with the use of the system model and system input. Then the system input is applied to the system and the actual configuration is measured. The difference between predicted and actual configuration is defined as:

$$\epsilon^{track}(k) := \|c_{target} - c(k)\|$$

Where c_{target} is the target configuration in the path that the controller tries to steer toward, and $c(k)$ is the actual configuration.

The Tracking Error can be described as:

A path consists of a list of configurations, a controller tracks the path by steering the system to the upcoming configuration in the path when reached the configuration is updated to the next configuration in the path. The difference between the current configuration and the current configuration the controller tries to steer toward is the TE.

c_{target} does not update every time step, whilst $c(k)$ does update every time step. As a result, a “good” TE is expected to take the form of a saw tooth function inverted over the horizontal x-axis.

Prediction Error (PE)	During executing a sudden high PE indicates unexpected behavior occurs, such as when the robot has driven into an object which it was not expecting. A high PE, which persists indicates that the robot is continuously blocked. Single collisions are allowed, but when the PE exceeds a pre-defined threshold and persists over a pre-defined time, the hgraph concludes that there was an error during execution and the edge failed.
-----------------------	--

Table 2.2: Monitor metrics used to monitor if a fault occurred during the execution of an edge

3

The Hypothesis and Knowledge Graph

This chapter is dedicated to introducing and defining the proposed framework, the proposed framework consist of the hypothesis algorithm, the hypothesis graph and the knowledge graph. The **hypothesis algorithm** acts on the **hypothesis graph** is responsible for searching the composite configuration space for action sequences to complete a specified task, Section 3.1.1 is dedicated to the halgorithm and the hgraph. The halgorithm additionally is responsible for collecting new knowledge of the environment. Gathered new environment knowledge is stored in the **knowledge graph**, defined in Section 3.2.1. Collected knowledge is rated and ordered from “good” to “bad” experiences using various metrics. Such an ordering within collected knowledge makes the kgraph a knowledge base that can be queried for action suggestions. Figure 3.1 presents a schematic overview of the interconnection of the knowledge-, hypothesis graph and the robot environment. A more in depth analysis of the hypothesis graph is given in Section 3.1, and for the knowledge graph in Section 3.2.

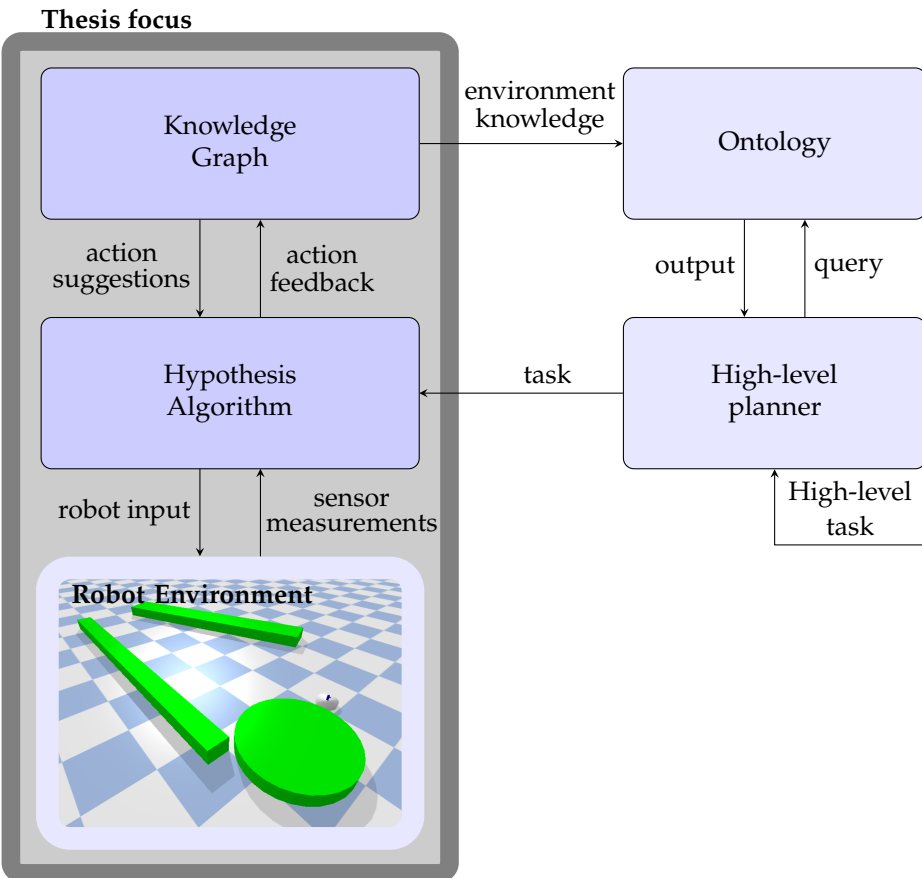


Figure 3.1: Flowchart representation of the proposed framework.

As the above figure shows, the thesis focus could be augmented with an ontology and high-level planner. Such an augmentation would create a framework capable of completing high-level tasks such as cleaning or exploring.

This chapter has terminology that is conveniently grouped in the following table.

Task:	Tuple of objects and target configurations. $\text{task} = S = \langle Obj_{task}, C_{targets} \rangle$
Subtask:	A single object, and a single target configuration. $\text{subtask} = s = \langle obj_{subtask}, c_{target} \rangle$
Object Class	Classification assigned to an object. $\text{OBJ_CLASS} = \text{Unknown} \vee \text{Obstacle} \vee \text{Movable}$
Node Status:	Status of a node indicates if a node is initialized, the halgorithm was able to bring the object to the configuration or whether the halgorithm fails to bring the object to its configuration.
	$\text{NODE_STATUS} = \text{Initialised} \vee \text{Completed} \vee \text{Failed}$
Node:	A node in the hgraph, represents an object in a configuration with reachability indicated with a node status. $\text{node} = v = \langle \text{status}, obj, c \rangle$
Edge Status:	Status of a edge, elaborate information on the statuses can be found in Figure 3.3.
	$\text{EDGE_STATUS} = \text{Initialised} \vee \text{PathExists} \vee \text{SystemModel} \vee \text{PathPlanned} \vee \text{Executing} \vee \text{Completed} \vee \text{Failed}$
Edge:	Edge connecting a node to another node in the hgraph or kgraph. $\text{edge} = e = \langle \text{status}, id_{from}, id_{to}, \text{verb}, \text{controller}, \text{dynamic model}, \text{path} \rangle$
Hypothesis:	Sequence of successive edges in the hgraph, an idea to put a object at it's target configuration. If executed and successfully completed, a subtask is completed. $\text{hypothesis} = h = [e_1, e_2, e_3, \dots, e_m], \quad m > 0$
Hypothesis Algorithm:	Graph based algorithm that searches for hypothesis in the hgraph to complete subtasks eventually completing a task.
Hypothesis Graph:	Collection of nodes and edges. For every subtask a start and target node exist in the hgraph, the halgorithm searches for a path through nodes and edges to connect start to target node. $\text{hgraph} = G^{hypothesis} = \langle V_H, E_H \rangle$
Knowledge Graph:	Collection of nodes and edges. The kgraph acts as a knowledge base and can be queried for an action suggestion. $\text{kgraph} = G^{knowledge} = \langle V_K, E_K \rangle$

Table 3.1: Terminology of terms used

3.1. Hypothesis Graph

The hypothesis graph (hgraph) consists of a set of nodes and edges. Where the node correspond to an object at a configuration, and the edges correspond to actions. As a whole the hgraph represents a

search (or planned search) in the composite configuration space. The halgorithm creates and updates nodes and edges in the hgraph and is discussed in Section 3.1.2. A search in the composite configuration space is avoided because an edge only operates in a single mode of dynamics, in the scope of this thesis a driving mode or pushing mode. The hgraph is created specifically for a task with a single start and a single target node for every subtask in the task. When the halgorithm halts and the task is completed, the hgraph is no longer needed and is discarded.

The halgorithm with the hgraph have a familiar structure compared to some recent literature [11, 40]. An important distinction is that the proposed framework in this thesis aims to combine the 3 topics: learning object dynamics, solving NAMO problems and nonprehensile pushing. Recent literature is able to only combine one or two topics of the three.

In the upcoming section the hgraph is defined and discussed in Section 3.1.1. The halgorithm is then discussed and in Section 3.1.2, where an explanation is provided on how the halgorithm searches for a solution in the composite configuration space. The section is concluded with an extensive example.

3.1.1. Definition

Before defining the hgraph, some definitions are defined on which the hgraph depends. First, recall the **configuration** defined in the Section 1.2.

Formally a **configuration**, $c_{id}(k)$ is a tuple of $\langle x(k), y(k), \theta(k) \rangle$
where $x, y \in \mathbb{R}$, $\theta \in [0, 2\pi]$

An object holds the information about an objects configuration and shape of the object.
Formally, a **object**, $obj_{id}(k) = \langle c(k), shape \rangle$

where $shape$ is linked to a 3D representation of the object, id is an identifier for the object.

An object node represents an object in a configuration.

Formally, a **objectNode**, $V_{id}^{obj} = \langle status, obj(k) \rangle$.

An edge describes the details of how a node transitions to another node in the hgraph. In the robot environment, an edge represents a change of configuration of an object. Edges are split into 2 categories, system identification edges that have as goal to collect IO data and generate a system model, and action edges that steer a system toward a target configuration. The different goals make action and system identification edges very different, which is why the distinction was made. At the same time the edges both represent a change in the environment as a result of the robot driving, pushing or collecting IO data. The edges are formally defined as:

A **identification edge**,

$$e_{(from,to)} = \langle status, id_{from}, id_{to}, \text{Identification Method}, \text{controller}, \text{input} \rangle$$

With id_{from} and id_{to} indicating the node identifier of the node in the hgraph where the edge start from and point towards respectively, identification method indicates the used method that converts IO data to a system model, the controller contains the control method used for driving the robot during the collection of IO data and input contains multiple sequences of input to send toward the system. For an identification edge it is important that it is compatible with the controller residing in the corresponding action edge.

A **action edge**,

$$e_{(from,to)} = \langle status, id_{from}, id_{to}, \text{verb}, \text{controller}, \text{dynamic model}, \text{path} \rangle$$

With id_{from} and id_{to} indicating the node identifier of the node in the hgraph where the edge start from and point towards respectively, verb an English verb describing the action the edge represents (driving, pushing), the controller contains the control method used for driving the robot, the dynamic model is the dynamic model used by the control method and the path a list of configurations indicating the path connecting a start- to target node.

Now the nodes and edges have been defined, the hgraph can be defined.

Formally, a **hypothesis graph**, $G^{hypothesis} = \langle V_H, E_H \rangle$ comprising $V_H = \{V_H^{obj}\}$, $E_H \in \{e_{(i,j)} | E_{Hi}, E_{Hj} \in \{V_H^{obj}\}, i \neq j\}$.

Most hgraph components have been defined. The status of an identification edge or action edge still remains undefined and requires some further explanation.

Status, Types and Lifetime of edges System identification and tracking a path are so very different, the edges are split into two categories, identification edges and action edges. An identification edge, which is responsible for sending an input sequence to the system and recording the system output. That IO sequence and assumptions on the system are the basis for system identification, techniques on various system identification methods are discussed in Section 2.1. The goal is to create a dynamical model which is augmented with a corresponding controller is closed-loop stable. The status of an identification edge can be visualized in the following Finite State Machine (FSM).

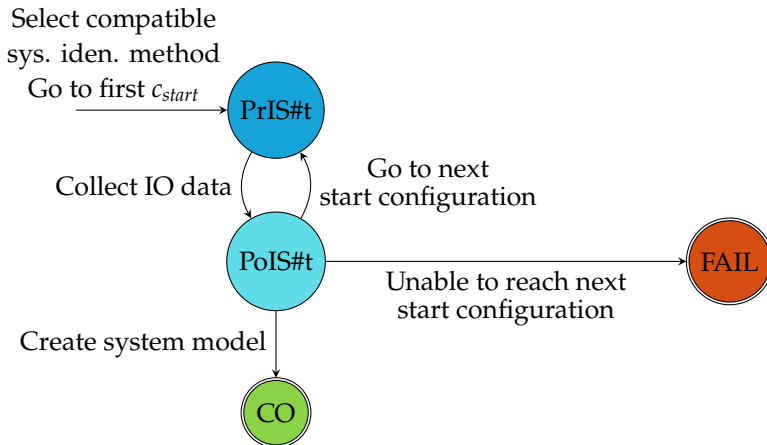


Figure 3.2: FSM displaying the status of an identification edge

PRE INPUT SEQUENCE number t (PrIS#t):	Go to target configuration to input the input sequence on the system.
POST INPUT SEQUENCE number t (PoIS#t):	Collect the output sequence.
COMPLETED (CO):	The edge has driven the system toward its target configuration and its performance has been calculated.
FAILED (FAIL):	An error occurred, yielding the edge unusable.

An identification edge corresponds to an action edge, because its goal is to generate an system model to then hand over its corresponding action edge. The system identification method is selected after the

action edge is selected such that the system identification method yields a system model compatible with the controller that resides in the action edge. Two types of system models generated, system models that describe the driving behavior of the robot, and system models that describe the push behavior of the robot and an object. Data collection for a driving model can be collected by sending input to the robot assuming that the robot has enough free space around it such that it does not collide with an object during data collection. To collect IO data for a pushing model the robot first drives to a starting configuration next to the object. After the first input sequence is over, the robot drives to the next start position next to the object. After several input sequences the robot has gathered enough IO data to generate a system model for pushing.

An action edge, contains a drive or push action. From the point of initialization an action edge starts collecting all necessary ingredients such that it can be executed (track a path). These ingredients are estimating path existence, being given a system model and searching for a path. To collect such ingredients the edge performs path estimation, is given a system model, performs motion or manipulation planning. Then finally, the edge is ready to be executed and send input toward the robot, an FSM of the action edge's status can be visualized in Figure 3.3.

Corrado: SOMewhere here must be an equation that if evolves to true, determines if a subtask was completed

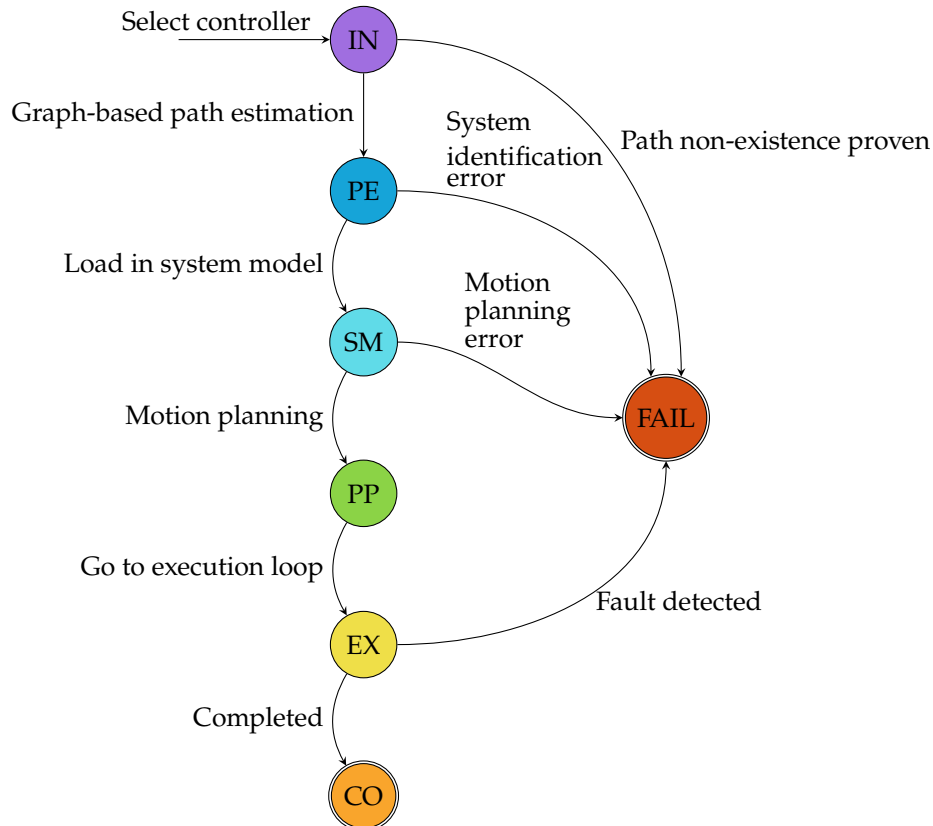


Figure 3.3: FSM displaying the status of an action edge

- INITIALIZED (IN): The edge is created with a source and target node which are present in the hgraph. A choice of controller is made.
- PATH EXISTS (PE): A graph-based search is performed to validate if the target configuration is reachable assuming that the system is holonomic.
- SYSTEM MODEL (SM): A dynamics system model is provided to the controller residing in the edge.
- PATH PLANNED (PP): Resulting from a sample-based planner, a path from start to target configuration is provided.
- EXECUTING (EX): The edge is currently receiving observations from the robot environment and sends back robot input.
- COMPLETED (CO): The edge has driven the system toward its target configuration and its performance has been calculated.
- FAILED (FAIL): An error occurred, yielding the edge unusable.

Figure 3.3 shows that many steps must successfully be completed before the edge can be executed. Before executing edges, edges must be initialized, which is where next section is dedicated to.

3.1.2. Hypothesis Algorithm

This section present and discuss the newly proposed halgorithm, this section will provide a mathematical description of the proposed halgorithm in the form of pseudo code. This section will discuss the search and execution loop that reside in the halgorithm and this section will finalize with 4 examples. First, let's look into the halgorithm pseudocode.

The halgorithm relies on a backward search technique. The backward search technique can be described as: *start the search at a goal state and work backward until the initial state is encountered [20]*. A motivation for a backward search over a forward search is that, it might be the case that the branching factor is large when starting from the initial state. In such cases, it might be more efficient to use a backward search.

<i>SubTaskNotFinished(s):</i>	Return False if the subtask s is completed or it is concluded to be unfeasible
<i>IsConnected(v_1, v_2):</i>	Return True if there exist a path in the hgraph from node v_1 to node v_2 through a number of non-failed edges
<i>ReadyForExecution(e):</i>	Return True if the edge e is ready to execute
<i>TargetNotReached(e):</i>	Return True edge e has not reached its target configuration
<i>FaultDetected(e):</i>	Return True if a fault has been detected during execution of edge e
<i>HandleFault(e):</i>	Update edge e status to FAILED and remove edge from hypothesis
<i>SteerTowardTarget(ob):</i>	Update controller with observation ob and compute response that steers the system to target configuration
<i>ReadyForExecution(e):</i>	Check if edge e has the PATH PLANNED status and contains all components to control the system
<i>incrementEdge:</i>	Mark current edge as completed, set next edge in h as current edge
<i>MakeReady(e):</i>	Perform actions to make the edge e ready for execution
<i>goBackward(v):</i>	Find the source node that points toward v through a number of non-failed edges
<i>findCorrespondingNode(v):</i>	Find the node containing the same object as v
<i>connectWithEdge(e_1, e_2):</i>	Randomly generate edge between nodes v_1 and v_2 or use kgraph to suggest an edge

Table 3.2: Functions used by the Algorithm 1

Algorithm 2 Pseudocode for the proposed hypothesis algorithm.

```

1: for  $s \in S$  do
2:   while  $\text{SubTaskNotFinished}(s)$  do                                ▷ Search Loop
3:     if  $G^{\text{hypothesis}}.\text{isConnected}(s.\text{start}, s.\text{target})$  then
4:       if  $h.\text{currentEdge}.\text{readyForExecution}$  then
5:         while  $\text{TargetNotReached}(h.\text{currentEdge})$  do                      ▷ Execution Loop
6:           if  $\text{FaultDetected}(h.\text{currentEdge})$  then
7:              $\text{HandleFault}(h.\text{currentEdge})$ 
8:             break
9:           end if
10:           $h.\text{currentEdge}.\text{steerTowardTarget}(ob)$ 
11:          if  $\text{TargetReached}(h.\text{currentEdge})$  then
12:            if  $\text{readyForExecution}(h.\text{currentEdge})$  then
13:               $h.\text{incrementEdge}$ 
14:            else
15:              break
16:            end if
17:          end if
18:        end while
19:      else
20:         $\text{makeReady}(h.\text{currentEdge})$ 
21:      end if
22:    else
23:       $v_{\text{localtarget}} \leftarrow G^{\text{hypothesis}}.\text{goBackward}(v.\text{target})$ 
24:       $v_{\text{localstart}} \leftarrow G^{\text{hypothesis}}.\text{findCorrespondingNode}(v_{\text{localtarget}})$ 
25:       $G.\text{connectWithEdge}(v_{\text{localstart}}, v_{\text{localtarget}})$ 
26:    end if
27:  end while
28: end for

```

During a backward search, edges are added pointing toward the target node (or to nodes that point toward the target node). Trying to connect the robot node through a list of successive directed edges to a target node. If such a path has been found in the hgraph, a hypothesis has been found and the robot can start executing edges.

A flowchart of the halgorithm is presented in Figure 3.4. Compared to the mathematical description of the halgorithm the flowchart provides more detail, including an elaborate description for every block in the flowchart (see Table 3.3). The flowchart includes path estimation, planning and the behavior when failure occurs. A connection point to the kgraph and robot environment are included. The blocks in the flowchart indicate which action they take and where, such as the configuration space, the kgraph or the hgraph. With the flowchart is straightforward to see how the halgorithm connects to the status of edges, with the mathematical description of the halgorithm that is harder so see. Compared to the flowchart the mathematical description is a abstracted version, leaving many details out that are related to the robot in this thesis. An abstracted mathematical description is simpler and encompasses a broader field of robots. So could the mathematical description also be applied to another robot such as a movable robot with robot arm and gripper. The flowchart encompasses to many details to be applied after such an change in robot hardware.

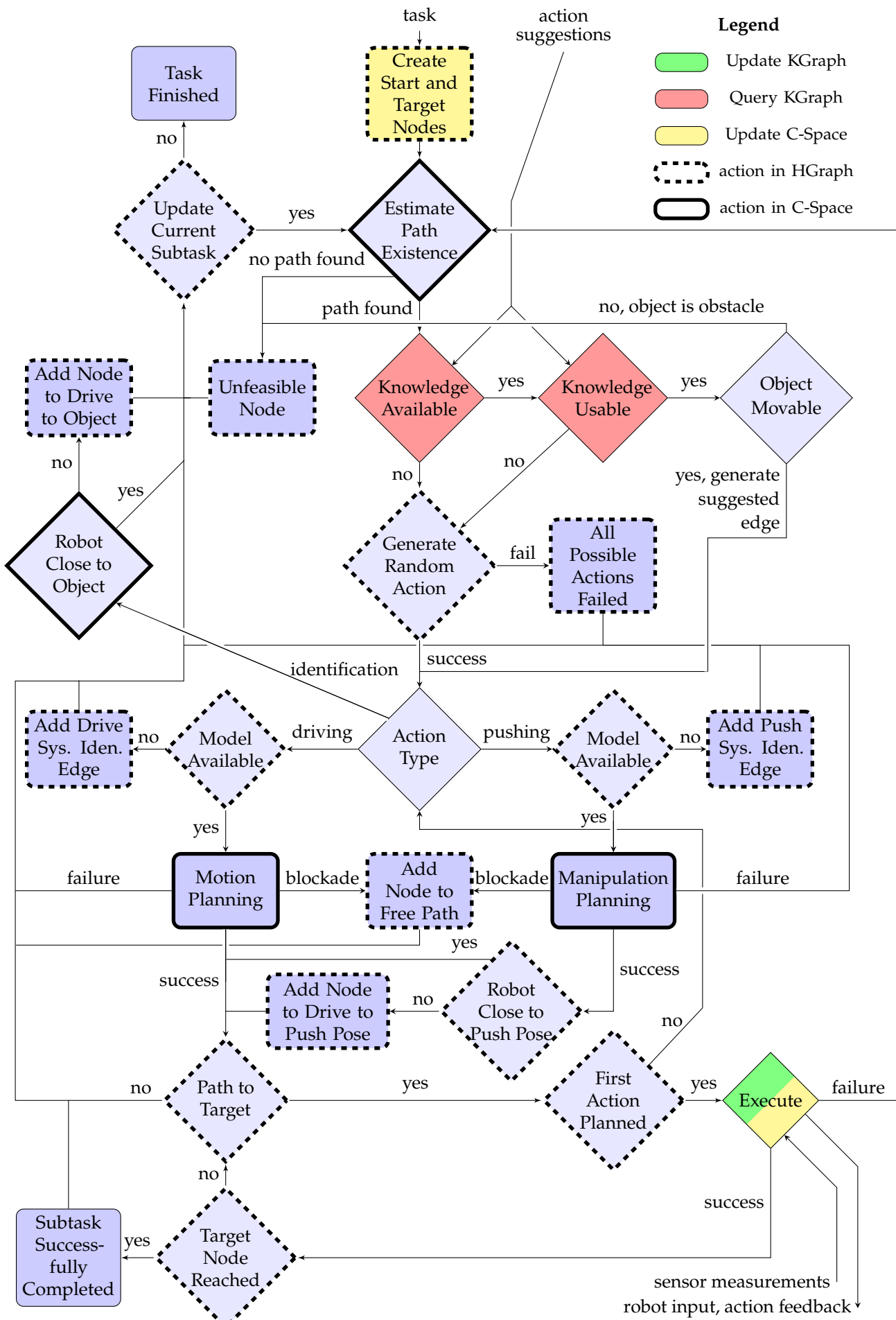


Figure 3.4: Flowchart displaying the hypothesis graph's workflow.

Node name	Description of actions taken
Task Finished	log all metrics for the hgraph, then deconstruct hgraph.
Create Start and Target Nodes	Generate a robot node and the start and target nodes for every subtask in the task.
Update Current Subtask	Select an unfinished subtask or update current subtask. Use the backward search technique. The <i>current_start_node</i> and <i>current_target_node</i> are updated. When all subtask have been addressed, conclude task is finished.
Estimate Path Existence	Check if a path exists between <i>current_start_node</i> and <i>current_target_node</i> whilst assuming that the object is holonomic.
Add Node to Drive to Object	Add a node before the <i>current_target_node</i> .
Unfeasible Node	Update node's status to unfeasible because is can not be completed, log failed Edge.
Knowledge Available	Query the kgraph for action suggestion to connect <i>current_target_node</i> to <i>current_target_node</i>
Knowledge Usable	Check if a suggested action is not on the blacklist.
Object Movable	Check if object is classified as movable
Robot Close to Object	Check if the object is inside directly reachable free space of the robot
Generate Random Action	Randomly sample a controller with a compatible system identification method that is not on the blacklist.
All Possible Actions Failed	Every possible action is on the blacklist for the <i>current_target_node</i> , update <i>current_target_node</i> status to failed.
Add Drive System Identification Edge	Adds identification edge between a newly generated node and the drive action edge source node.
Model Available	Checks if the drive action edge contains a system model.
Action Type	Checks the action type.
Model Available	Check if the push action edge contains a system model.
Add Push System Identification Edge	Adds identification edge compatible with push action edge.
Motion Planning	Search a path for the <i>current_edge</i> , detect blocking objects.
Add Node to Free Path	Search close by pose for object to free path. Create node to push object toward that pose.
Manipulation Planning	Search a path for the <i>current_edge</i> , detect blocking objects.
Add Node to Drive to Push Pose	Create node to drive toward push pose, add before action edge.
Robot Close to Push Pose	Check if the robot is overlapping with the best push position.
Path to Target	Is there a path from robot to target node in the hgraph, then set first edge to <i>current_edge</i> otherwise update subtask.
First Action Planned	Check if motion/manipulation planning was performed.
Execute	Execute the <i>current_edge</i> , update hgraph after completion, log failed hypothesis if a fault is detected.
Subtask Successfully Completed	Log hypothesis metrics.
Target Node Reached	Check if the target node is reached.

Table 3.3: Elaborate information on actions taken by blocks in Figure 3.4.

When all tuning parameters are set, the hgraph is initialized and a task is provided, there is only a single access point toward the hgraph. A function $respond(observation)$ that provides the halgorithm with sensor measurements of the environment with the argument $observation$. The function $respond(\cdot)$ returns control in put for the robot. In this theses, the sensor measurements are the configuration of objects in the environment. Recall that the perfect-sensor assumption, assumption 1.2.2 that makes access to the exact configuration of every object possible.

The Blacklist An failed edge is labeled as failed, then is could be regenerated again. Entering an infinite loop of being generated, failing, being labeled as failed and being generated again. Such behavior is undesirable and is prevented by the blacklist. The blacklist prevents certain edge parameterization to be generated to reach a specific node in the hgraph. When two nodes are connected with an action edge, the possible parameterizations are filtered. Thus any parameterization that is on the blacklist for this specific node (to which the action edge would point toward) cannot be created again for the lifetime of the hgraph. An example where the blacklist can be seen in action is Figure 3.11.

3.1.3. The Search and the Execution Loop

In Figure 3.4 two main loops can be identified, see Figure 3.5. These loops are the search loop, and the execution loop.

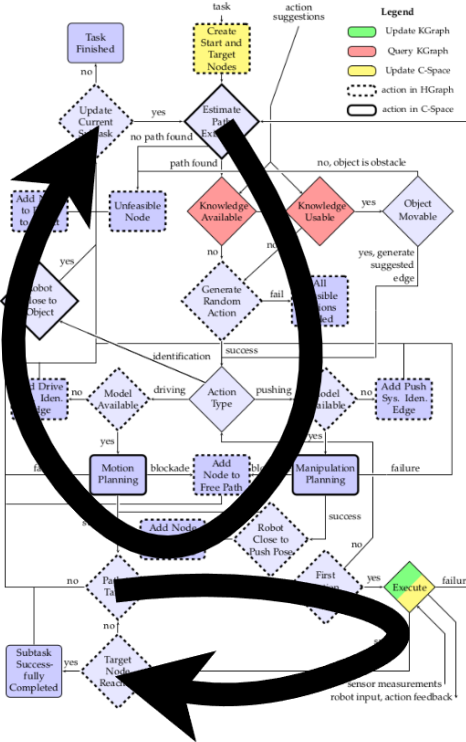


Figure 3.5: The search (above) and execution (below) loop.

Whilst the halgorithm resides in the search loop, hypotheses are formed. Forming a hypothesis generates nodes, edges, and progressing their status as described in Figures 3.2 and 3.3. In the execution loop *an edge is being executed*, a phrase to describe that the controller residing in an edge is sending control input toward the robot. The halgorithm operates synchronously, thus at any point in time, the halgorithm resides in a single block within Figure 3.4. The result is that the robots cannot operate whilst the halgorithm resides in the search loop, and during execution, no hypothesis can be formed or updated. Assumption 1.2.2 guarantees that the robot environment does not change causing existing

hypotheses to be outdated.

3.1.4. Examples

Before displaying example hgraph's a legend is presented below.

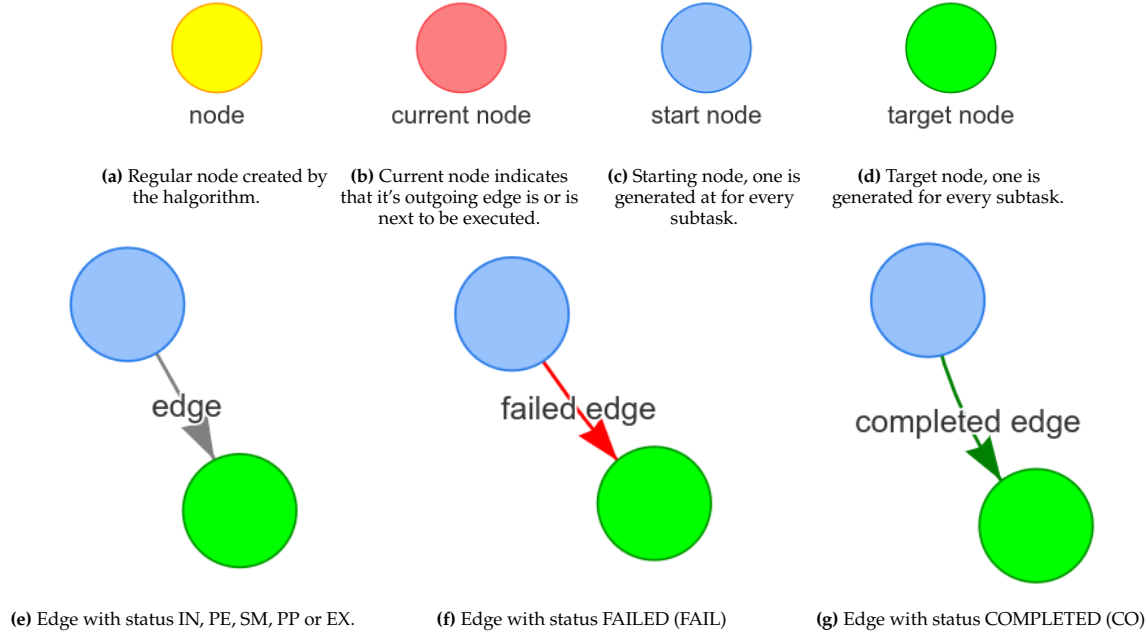


Figure 3.6: Legend for hgraph's nodes and edges

Driving and Pushing Four examples are presented, starting with a driving task in Figure 3.7, then a pushing task in Figure 3.9.

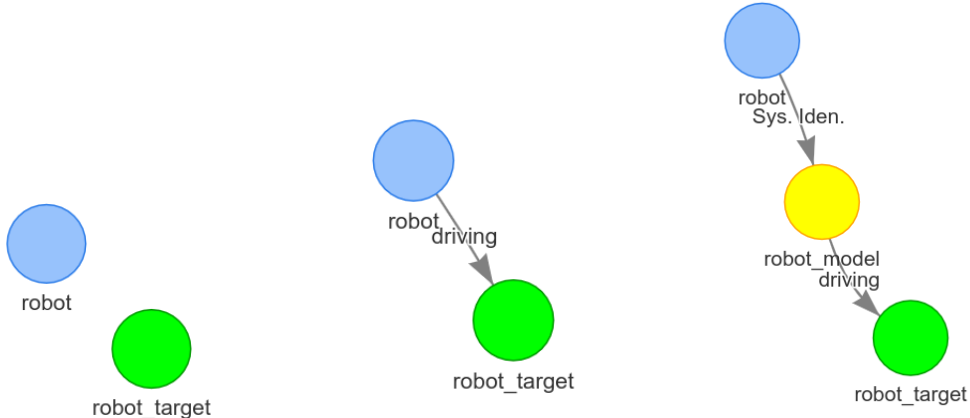


Figure 3.7: hgraph generated by the halgorithm to drive the robot to a target configuration

The robot does not have a system model of itself, thus first system identification must be performed before it can drive to the specified target configuration. The kgraph that will be discussed in Section 3.2.1 can suggest an action that includes a system model. In that case, system identification is not needed. The following figure displays successfully executing the hypothesis found in Figure 3.7.

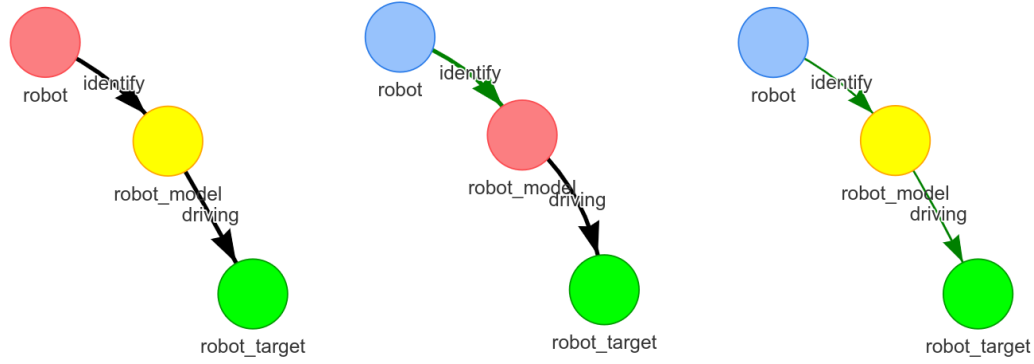


Figure 3.8: Executing the hypothesis found in Figure 3.7.

Upcoming figure will display the hypothesis generated to push an object to a target position. Both generating a hypothesis and executing the hypothesis are intertwined, this is because certain information should first be collected from the environment before the full hypothesis can be generated. An example is the *best_push_position* that can be found in Figures 3.9g to 3.9i. The *best_push_position* can be found after manipulation planning for the pushing edge is completed. For motion planning a system model is required, thus the corresponding system identification edge should be completed before manipulation planning can start, and than the *best_push_position* can be determined.

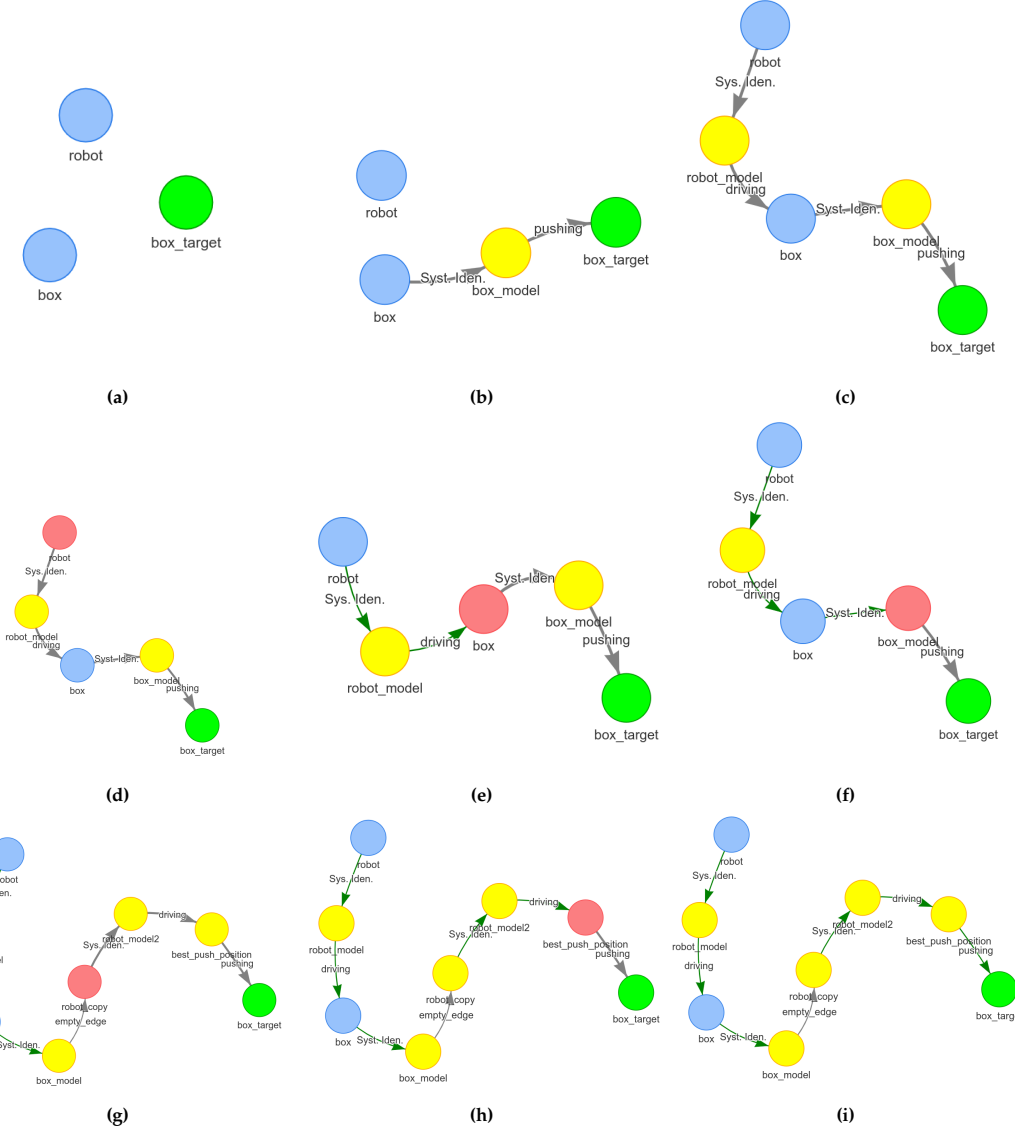


Figure 3.9: hgraph for pushing the green box to the target configuration

Especially in Figures 3.9b and 3.9c the backward search is clearly visible, the halgorithm searches from target node to the robot node. Figure 3.9 is extensive because every necessary steps is included whilst some could be skipped. First, identifying a system model for robot driving twice, if the system model created in edge Sys. Iden. pointing toward node robot_model is reused, then the edge Sys. Iden. pointing toward robot_model_1 would be unnecessary. Second, if system models would already be available for driving and pushing, no single system identification edge would be required. A *empty_edge* can be seen in Figures 3.9g to 3.9i, the *empty_edge* serves to connect a node to another node (box_model to robot_copy in Figure 3.9). The *empty_edge* can be traversed without execution, holds no controller, system model or status.

Encountering a Blocked Path During propagation of an action edge's status, motion or manipulation planning occurs. If an object is blocking the path, planning will detect it and the halgorithm tries to free the path. In the next example the halgorithm detects a blocking object and frees the path by pushing the blocking object to a new configuration, and can be visualized in Figure 3.10.

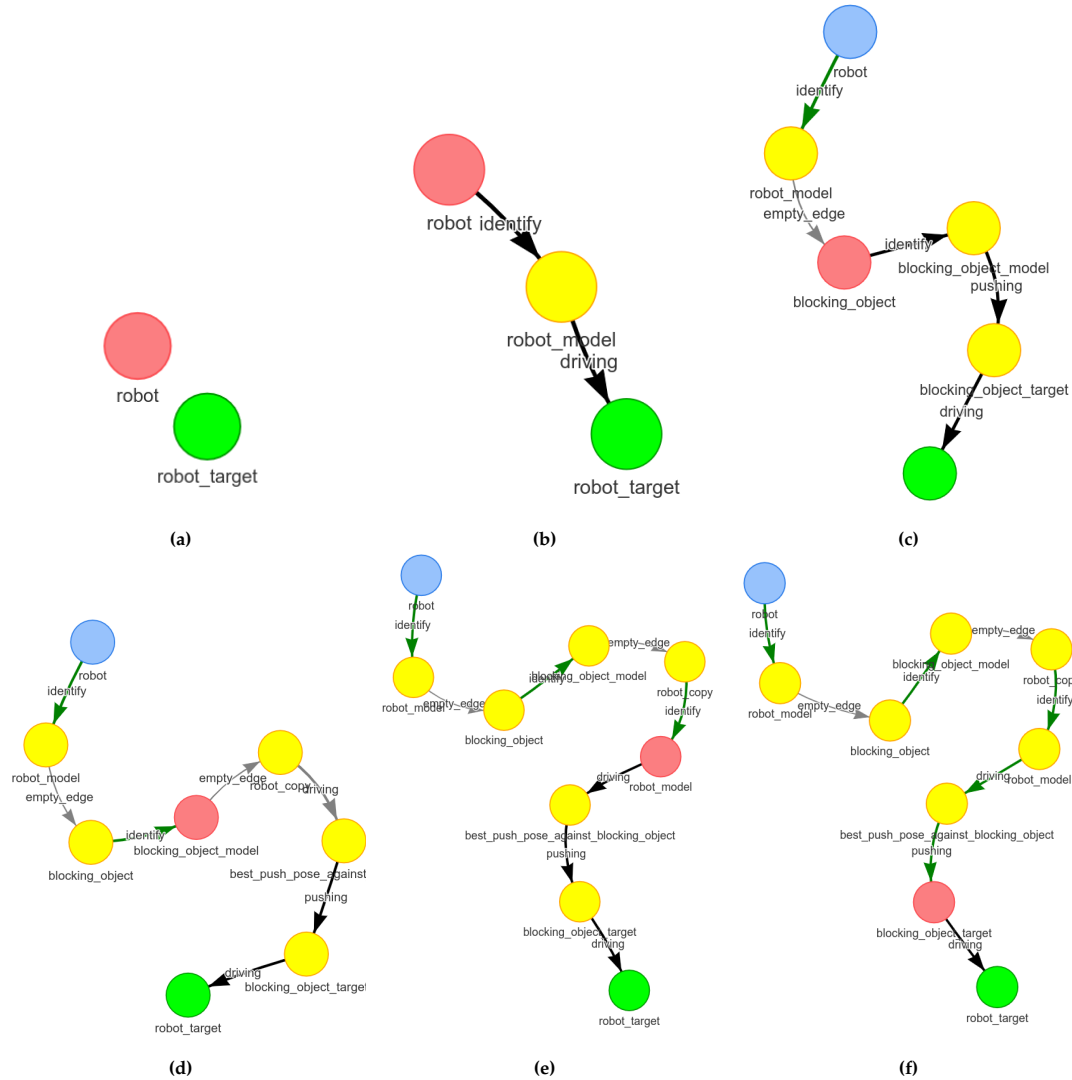


Figure 3.10: hgraph for driving to target configuration and encountering a blocked path

Encountering Failure In the last example, the first hypothesis fails to complete and the halgorithm tries to generate a new hypothesis that also fails to complete. Several faults and failures are modeled, the halgorithm response to faults and failure is the same. If during the propagation of an edge's status any kind of failure arises, the failed edge and corresponding edges are marked as failed. Equally during execution, if a fault is detected, the execution halts and the edge and corresponding edges are marked as “failed”, the procedure can be seen in Figure 3.11.

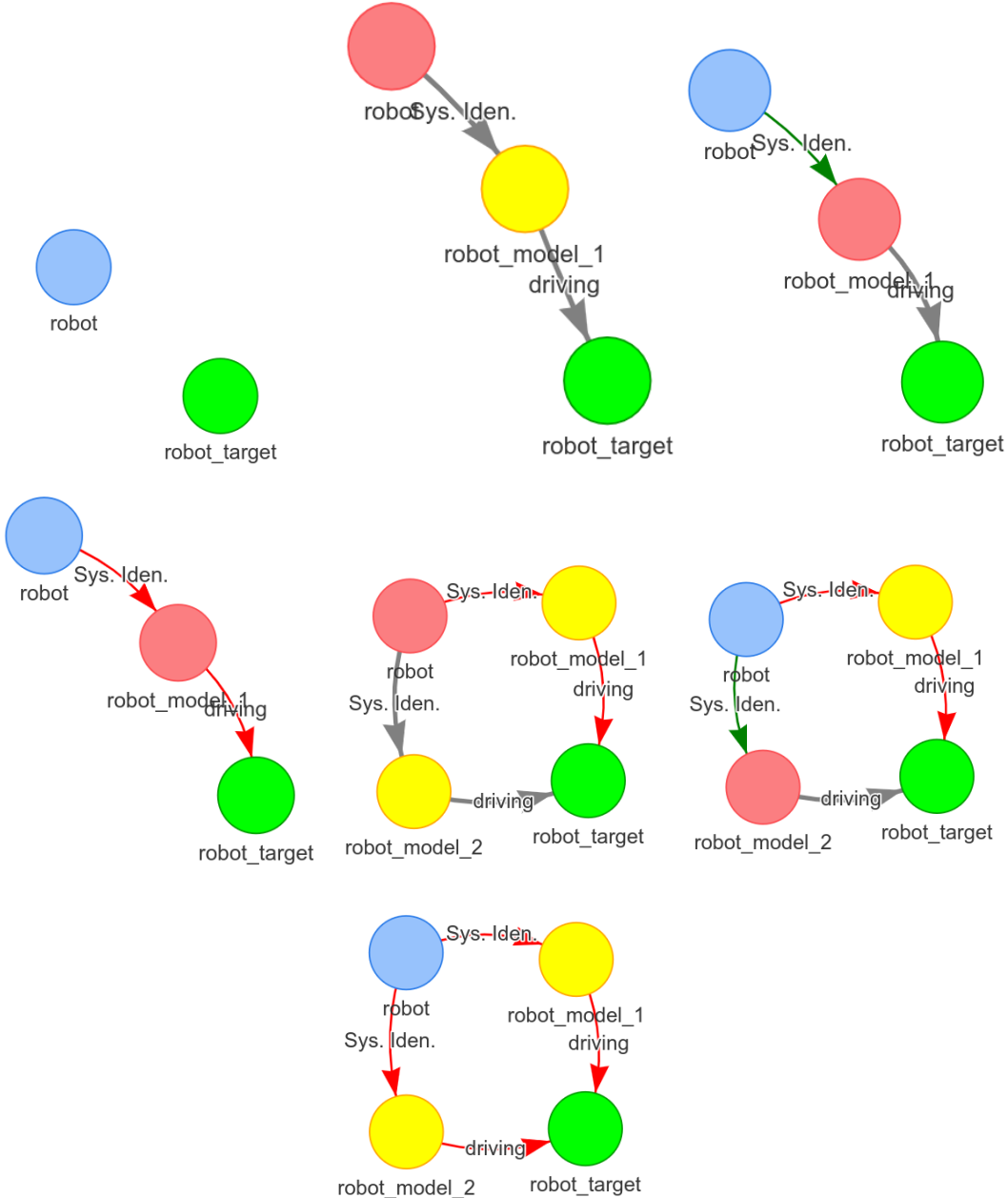


Figure 3.11: Executing two hypothesis, both failing to complete because a fault of failure emerged.

In Figure 3.11 only two parameterizations of drive controller and system model were available. Thus after two failed hypothesis the halgorithm concludes it cannot complete this task.

What by now hopefully became clear to the reader is that the halgorithm autonomously searches for hypotheses in the hgraph to solve a task, one subtask at a time. The halgorithm switches between the search and execution loop. Switching from the search loop toward the execution loop when a hypothesis is found, and switching back when a hypothesis is completed or a fault or failure occurred.

The limited number of possible edge parameterization (every combination of a system identification method with a compatible control method) guarantees that the robot tries to complete a subtask, but concludes that it is unable to complete a subtask if all possible edges have failed.

Recall the 3 topics (learning object dynamics, the NAMO problem and nonprehensile push manipu-

lation) that this thesis proposes to combine. The halgorithm can solve NAMO problems because the robot can drive toward target positions even if reaching such a position requires objects to be moved first. The halgorithm can push objects to target positions by first identifying a system model and then pushing the object toward its target position. The proposed algorithm learns to classify objects by updating objects class from unknown to movable or obstacle. The system model that system identification yields is however of short use, it is only given to the corresponding action edge. In the next section, the edges that are executed will be reviewed and stored in a knowledge base. The knowledge base will suggest a parameterization for an edge when faced with similar nodes to connect.

3.2. Knowledge Graph

The hgraph discussed in previous section has a lifetime that spans over a single task, learned system models are not stored for hgraph that are created for future tasks. Storing learned environment knowledge is the kgraph's responsibility. Another responsibility of the kgraph is to make an ordering in the stored environment knowledge. The ordering is made with a proposed success factor, a metric that combines multiple metrics such as prediction error, tracking error and the success-fail ratio of a edge parameterization (controller and system model).

The name "knowledge graph" originates from the environmental knowledge it contains, and its graph structure. Both the hgraph and kgraph are newly proposed frameworks build from the ground up, with only inspiration from an already existing technique, a backward search. The kgraph does not adhere to any standard that may apply to standardized knowledge bases.

3.2.1. Definition

Before defining the kgraph, some definitions are defined on which the kgraph depends, such as the success factor, center and side nodes and edges.

$$\text{Formally the success factor, } \alpha = \begin{cases} (0.5 - \epsilon_{\text{avg}})^{1 - \frac{N_{\text{success}}}{N_{\text{fails}} + N_{\text{success}}}} & \text{if } \epsilon_{\text{avg}} < 0.4 \\ 0.1^{1 - \frac{N_{\text{success}}}{N_{\text{success}} + N_{\text{fails}}}} & \text{if } \epsilon_{\text{avg}} \geq 0.4 \end{cases}$$

The success factor is discussed in upcoming paragraph.

An edge describes the parameterization that it holds, and how that parameterization compares to other edges in the kgraph.

$$\text{Formally an edge, } e_{(from,to)} = \langle id_{from}, id_{to}, \alpha, \text{System Model, Controller} \rangle$$

Where (System Model, Controller) together is referred to as edge parameterization.

An center node is linked to an object that is its main task.

$$\text{Formally, a center node, } v_{id}^{\text{center}} = \langle id, obj_{id}, \text{OBJ_CLASS} \rangle$$

Where id an identifier for the center node, obj_{id} an identifier linked to an object, OBJ_CLASS the classification of that object.

A side node represents nothing, it is a placeholder for the edge to point toward.

$$\text{Formally, a side node, } v_{id}^{\text{side}} = \langle id \rangle$$

Now the nodes and edges have been defined, the kgraph can be defined.

$$\text{Formally, a knowledge graph, } G^{\text{knowledge}} = \langle V_K, E_K \rangle \text{ comprising } V_K = \{v^{\text{center}}, v^{\text{side}}\}, E_K \in \{e_{(i,j)} | i \in E_{K_{ids}}^{\text{center}}, j \in E_{K_{ids}}^{\text{side}}\}.$$

Where $E_{K_{ids}}^{center}$ and $E_{K_{ids}}^{side}$ are the identifiers of the set of center edges and side edges respectively.

Now the kgraph is defined, lets investigate an example.

Success Factor The responsibility of the kgraph is to collect and suggest edge parameterizations. Estimating which parameterization would be the best candidate is an entire field of research on its own. So could action suggestions incorporate uncertainty, specific parameterizations can be suggested with the goal of collecting feedback on them. Or even suggest a parameterization based on the feedback on other parameterizations [18]. A simple metric, the success factor has been chosen, based on the average prediction error and the number of times an edge succeeded or failed. From the point of the kgraph there is little information to work with, feedback must be created with only information on prediction error, tracking error and weather there was a fault detected. Then action suggestions must be made based on collected feedback and an object that should change start configuration to a target configurations (connecting 2 nodes in the hgraph). A simple success factor thus already incorporates most of the available metrics.

success_factor =

$$\begin{cases} 0.1^{\epsilon_{avg}} & \text{if edge does not yet exist in kgraph} \\ \text{success_factor} + 0.1 * (1 - \text{success_factor}) & \text{if success_factor already exist in kgraph} \\ & \text{and edge was successfully completed} \\ \text{success_factor} - 0.1 * \text{success_factor} & \text{if success_factor already exist in kgraph} \\ & \text{and edge failed} \end{cases}$$

The kgraph has 3 important functions. The *add_object* function adds object information to the kgraph, important for adding unmovable obstacles that cannot be manipulated by the robot. The *add_review* function is used when an edge successfully completed or failed, the corresponding node in the kgraph is updated with a new success factor as described in the formula above. The *action_suggestion* returns the best parameterization it contains for an object.

3.2.2. Example

An example kgraph can be visualized in Figure 3.12, the parameterization of edges is displayed and the object that the edge controls as image. For clarification, the connected left part with image of the point robot on the center node has 3 outgoing edges that describe robot driving. The connected part on the right with an image of the point robot and the green box on the center node has 2 outgoing edges that describe robot pushing against the green box.

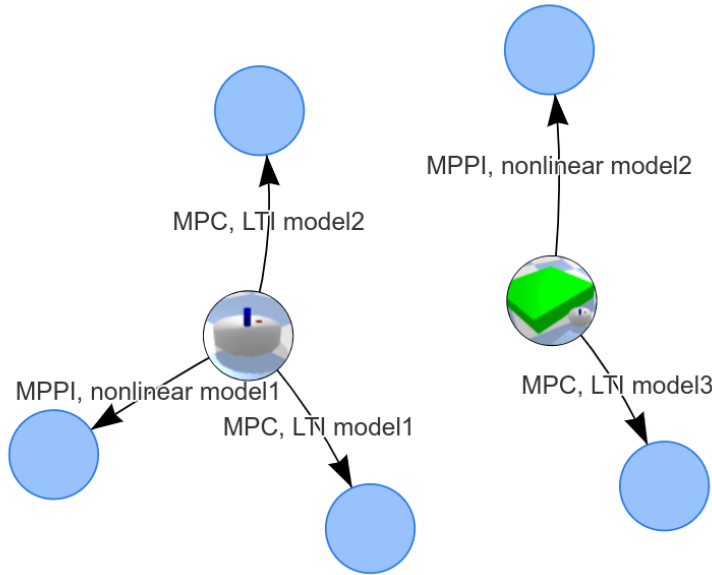


Figure 3.12: kgraph with 3 edges on robot driving, and 2 edges for pushing the green box.

The edges in the figure above display only the edge parameterization, but store more information, mainly the success factor. The blue nodes serve a small purpose, making sure edges can point to a node. The blue nodes could fulfill a larger purpose, that is describing which actuators the edge can control. For example, a mobile robot with robot arm attached can have a set of controllers that only drive the base, a set of controllers that only steer the robot arm and a set that controls both the base and robot arm. In such cases the blue nodes describe which part of the robot can be actuated. The controllers considered in this thesis control every actuator of the robot, resulting in the blue nodes serving such a small purpose.

3.2.3. Edge Metrics

The kgraph keeps an ordered list of ‘good’ and ‘bad’ edge arguments (controller and system model). ‘Good’ and ‘bad’ are defined by edge metrics, these metrics are created after the completion of an edge, regardless of whether the edge was successfully completed or failed. An indication is given on why certain metrics matter in Table 3.4.

Prediction Error (PE)	To better compare prediction errors the PE is summarized and average PE. The average PE is an indicator of an accurate system model but can give misleading results since PE is also an indicator of unexpected collisions. Prediction error should thus only be used if there are no collisions detected. The average PE comes with more flaws since the average is mostly determined by outliers, some unfortunate outliers in the PE might for the largest part determine the average PE. The average PE will thus not be used because it is not robust enough.
ratio num_successfully completed edges and num_total edges	Over time the kgraph can recommend the same edge arguments multiple times. Logging the ratio of succeeding edges vs total edges builds an evident portfolio. Still, this metric has to be taken with a grain of salt because edges with equal edge arguments perform similar actions e.g. pushing an object through a wide corridor is compared to pushing the same object through a narrow corridor. One could say "comparing apples with pears".
the final position and displacement error	The quality of the result is measured in the final position and displacement error. The importance should thus be stressed when ordering edge arguments.
planning time	With system identification, path estimation, motion or manipulation planning the planning time can vary in orders of magnitude between simple or more complex approaches. Planning time mainly serves to rank the slowest planners low, whilst not influencing the rank of fast and average planners.
run time	Also known as execution time would be a quality indicator if start and target states would be equal. Edges are recommended to solve similar tasks, where the path length between the start and target state is different. Thus planning time is not of any use to rank edges.
completion time = run time + planning time	With the same argumentation as run time, completion time is not of any use to rank edges.

Table 3.4: Edge metrics used to rank control methods from 'good' to 'bad'

The kgraph fulfills two goals. It stores information whether an object can be manipulated, and stores an ordered list from most successful control and system model combination to least successful per object. Information if objects can be manipulated prevent hypothesis from trying to push unmovable objects. A list of most successful control and system model combinations will suggest the best possible combination to fulfill the drive of pushing action.

4

Results

*This chapter presents the test results that test and challenge the proposed framework. The randomization tests, which additionally test the influence of the kgraph and test taken including and excluding the kgraph. The test results provide evidence that supports the effectiveness of the proposed framework. This chapter starts by introducing **method metrics** that indicate how a task has been executed by the proposed framework in Section 4.1. A comparison is made with the state-of-the-art methods in Section 4.3.*

The Simulation Environment Testing in a simulation environment has been done using the URDF Gym Environment [33], a 100% python environment build upon the PyBullet library [7]. The code created during the thesis can be found on GitLab and GitHub. Experiments ran on standard TU Delft laptop: HP ZBook Studio x360 G5, running OS: Ubuntu 22.04.1 LTS x86_64, CPU: Intel i7-8750H (12) @ 4.100GHz, GPU: NVIDIA Quadro P1000 Mobile. The simulation environment provides many different

robots, of which two simple robots are selected to perform tests, they are displayed in Figure 1.1, and various objects are displayed in Figure 1.2.

4.1. Proposed Method Metrics

Corrado: I'm confused, what metric is exactly used? Write it explicitly, GIJS: first sentence here

The results are measured in method metrics, not to be confused with the monitoring metrics in Section 2.4 or the edge metrics in Section 3.2.3. The results are interesting, but most interesting is the progression of the method metrics over time. As will be shown, the effect of learning can be measured by investigating and tracking the method metrics over time. Furthermore, the method metrics will be used to compare the proposed framework to relative state-of-the-art papers. First, the method metrics are presented in Table 4.1 with corresponding argumentation on the relevance of the metric.

Corrado: I'm very confused by what metric is used for what part and why some metric (from earlier) are not used but still presented

Total Average Prediction Error	The total average PE is calculated by augmenting every prediction error into a single list, then the mean and standard deviation are calculated over that list. Since the PE is high when unexpected behaviour occurs, seeing the total average PE lower would indicate the robot encounters less unexpected behaviour, indicating the robot is learning.
The ratio between the number of hypotheses and the number of tasks	Expected is that whilst learning system models, the hypothesis created will be more effective. Thus the ratio between the total number of hypotheses and the total number of tasks is expected to lower with new knowledge.
The ratio between the number of successful and the number of total edges in kgraph	When the kgraph improves recommending a controller and system model, the ratio between successful edges and total edges is expected to increase because, with better recommendations, more edges will be completed.
task completion time = run time + planning time	If equal tasks are given multiple times, the total task completion time should drop pretty drastically. Multiple factors help to lower the task completion time, firstly system identification has to be performed only once, and there is no need to lose time on redoing system identification. Secondly, the hgraph is expected to improve generated hypothesis, or better said, the same mistake should not be made multiple times, resulting in fewer failing hypotheses and lowering task completion time.

Table 4.1: Proposed method metrics used to compare the proposed framework with the state-of-the-art.

Three system models are used for testing. The goal of this thesis is not to find optimal control, or to model the environment very accurately. The goal is to select the best combination of controller and system model in the available set of controllers and system models. Only a short textual description of the available system models is provided below.

Martijn: you don't explain what these models are, nor do you re-use these model names anywhere in the thesis.

<i>lti-drive-model</i>	A second order LTI model that can be used by both the MPC and the MPPI drive controller. The next robot configuration is based on the current configuration and system input in x and y direction.
<i>nonlinear-push-model-1</i>	A nonlinear model describing the next object configuration in x and y direction and the orientation θ based on the current configurations of the robot, the object and on the robot inputs in x and y direction.
<i>nonlinear-push-model-2</i>	A nonlinear model describing the next object configuration in x and y , and the object configuration in x and y direction based on the current configurations of the robot, the object and on the robot inputs in x and y direction.

Table 4.2: Available drive and push system models used for testing.

Corrado: Missing the details. You need to add these models in order for someone to be able to reproduce the results or at least understand them GIJS: Add the formula's for these models

4.2. Randomization

In the randomized environment, the robot is tasked to push a number of objects to a target location. The randomized environment provides a more unbiased result. The random environment does not deliver completely unbiased results because several parameters must be chosen to create and set up the random environment, which are.

Corrado: above sentence feels contradictory

Corrado: For every plot put the control parameterisation on every plot!

The <i>size of the grid</i>	in x and y direction.
The <i>minimal and maximal size of objects</i>	A box will have sides with a length that lie in the specified range from minimal to maximal length. Cylinders will have a diameter and height that is within the specified range, additionally, cylinders are not higher than the radius of the cylinder to prevent cylinders from tipping over.
The <i>maximal weight</i>	which is uniformly distributed for the environment objects, minimal weight is set by default to 1.
The <i>number of unmovable objects</i>	Specify the amount of unmovable objects.
The <i>number of movable objects</i>	Specify the amount of movable objects.
The <i>box or cylinder object</i>	For every new object generated there is a 50% chance it becomes a box and 50% chance it becomes a cylinder, letting randomization determine the ratio between boxes and cylinders.
The <i>number of subtasks in a task</i>	Specify the amount of subtasks in a task.

If the task is completed, a *reshuffle* function reshuffles the objects in the environment, that is the objects remain the same objects, but the objects receive a new initial position, and the subtask target configurations are renewed. The reshuffled environments can be seen in Figure 4.2.

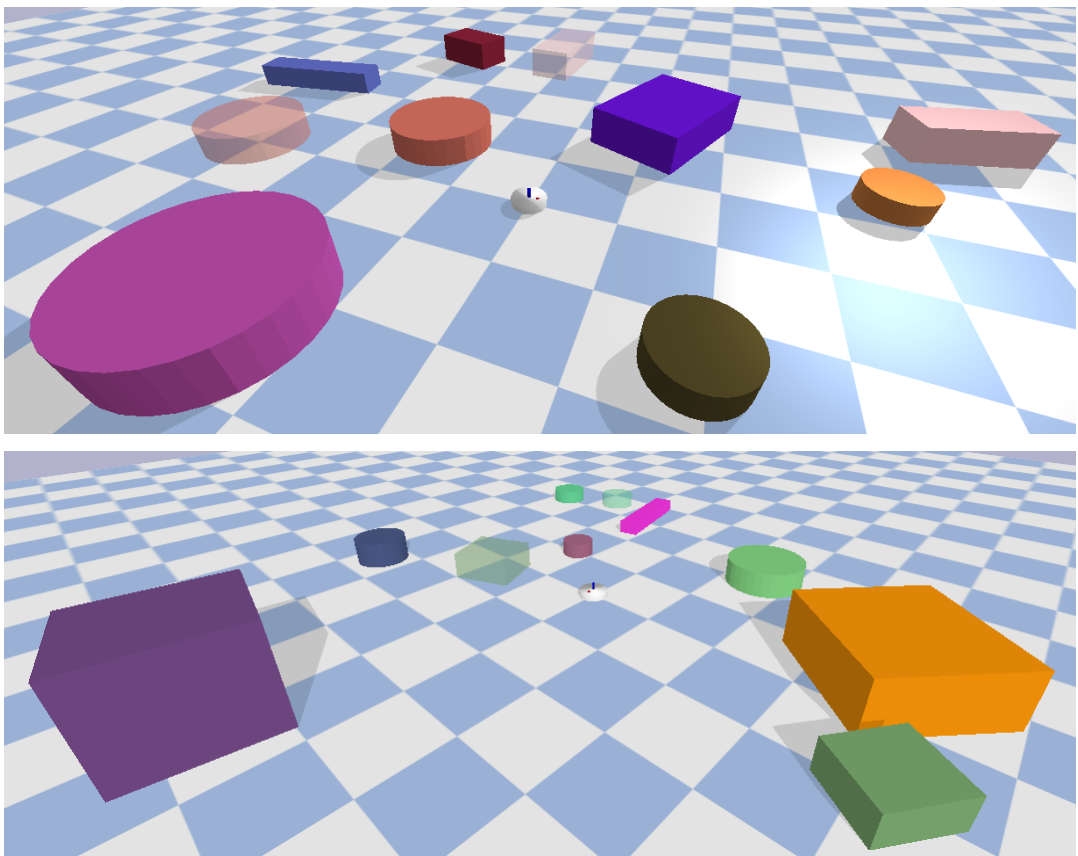


Figure 4.1: Two random environments with 2 target ghost configurations for the task containing 2 subtasks.

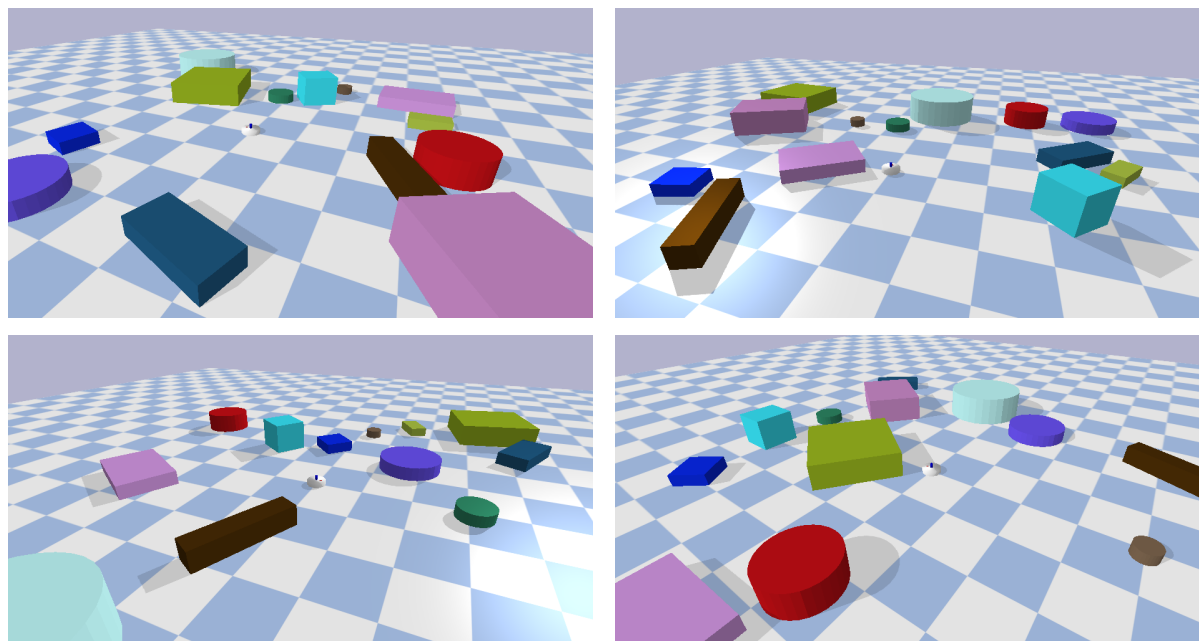


Figure 4.2: A random environment that is reshuffled 4 times. Target ghost configurations are not shown.

The halgorithm will be tested with both driving and pushing tasks. Starting with driving tasks for which the parameters are set to be.

add to the table below: max speed = 1.0, known obstacle cost = 2, unknown obst cost = 3.5

grid size	$x = 12m, y = 12m$
object size	$min_length = 0.2m, max_length = 2m$
object weight	$max_weight = 1000g = 1kg$
number of objects	$num_unmovable_obj = 3, num_movable_obj = 5$
number of subtasks	$num_subtasks = 3$

These parameters have been specifically selected, starting with the size of the ground floor. The ground floor should be large enough such that objects can be pushed around, note that, for a driving task, pushing is involved when a path must be freed. Environments must thus not be too small. A ground floor too large would result in a longer computational time for path estimation and planning which is undesired. A 12 by 12 is selected because it is reflecting a reasonably large workspace, whilst computation times for planning are kept similar to computation times

Corrado: sentence above is unclear

. The range that determines the size of objects is set such that objects can be as large as the robot itself, and be around 10 times as large as the robot. With these sizes the robot is unable to grasp objects, a gripper would be too small to grasp objects. The comparatively large size fits the objective of nonprehensile pushing, there simply is no other method to manipulate such large objects other than pushing. A real-life example are can be found in harbours where tug boats push giant cargo ships around that are many times over the size of the tug boat. The ratio of solid obstacles vs. movable objects determines if a task is more navigation (only solid obstacles) or more NAMO (only movable objects). A task that tends toward NAMO is favoured because that is the target environment in this thesis. There should be some unmovable obstacles that reward the robot learning such objects are unmovable (to then not interact with them). Thus there are more movable objects than solid obstacles chosen, whilst still having 2 solid obstacles around. The number of subtasks is set to 3, a low number of drive subtasks that can be completed in under 2 minutes.

The following figure shows a driving task containing 3 subtasks for the robot, which translates into driving to three target configurations. The randomly generated task in the random environment is reshuffled and then solved 10 times. The sequence of tasks is performed with the kgraph suggestions.

Corrado: What are these suggestions?

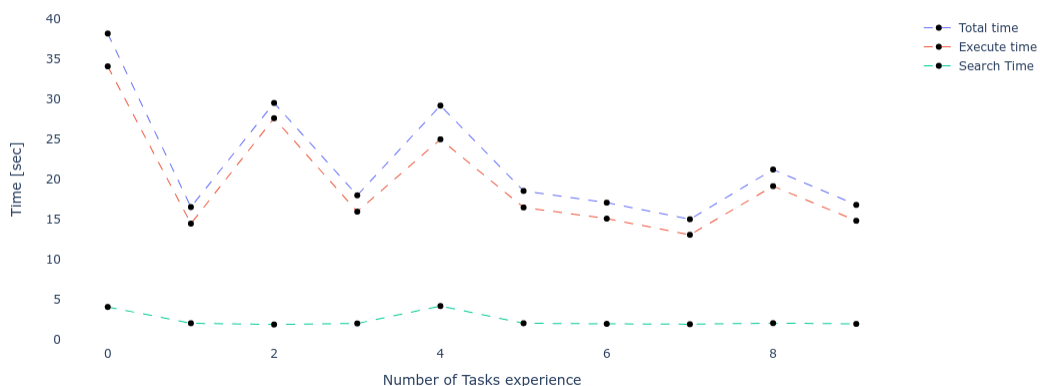


Figure 4.3: Robot tasked to drive toward 3 target configurations, the environment is reshuffled after completing a task.

Martijn: To do that properly, you should have done so many experiments that this influence of random path lengths is averaged out. Gijs: reach statistical relevance please

Corrado: Show this in a graph. There is no mention to MPC or mpfi in the graph make such a graph!

What is not shown in the above figure is that the kgraph over times prefers the MPC controller over the MPPI controller (both using the *lti-model-1*) because of its lower average prediction error. The MPC controller is a bit faster compared to the MPPI controller thus the execution time decreases over time. The execution time is strongly correlated with the path length because driving to a target further away takes longer. It is thus only useful to investigate the trend that Figure 4.3 and not individual data points.

Corrado: How are the suggestions built? Add a numerical example

Then the same environments and tasks are solved 10 times without the kgraph suggestions. The randomly generated tasks and environments are repeatable by fixing the seed. The fixed seed ensures that the randomly generated environments can be created multiple times, once to solve with kgraph suggestions and once to solve without help from the kgraph.

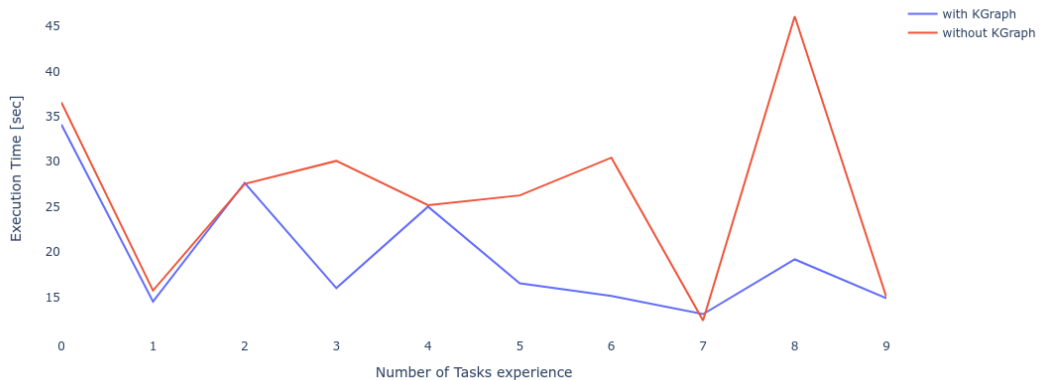


Figure 4.4: Execution times for driving toward target configurations with and without kgraph.

Martijn: It is unclear what this image presents atm, and: If you repeat the experiment, will the graph look completely different?

The figure above shows similar running times at the first few solved tasks. During these first tasks the kgraph

Corrado: How exactly

is filled with edge feedback, but the kgraph has not gained enough feedback to suggest action parameterizations, this period can be referred to as the learning phase. After this learning phase, the kgraph suggests the MPC controller over the MPPI controller, because of its relatively higher success factor

Corrado: You need to show these values otherwise it's very vague

. The action suggestions improve overall execution time, note that selecting random controllers can result in equal execution time. In these cases, (4, 7 or 9 tasks in experience in figure 4.4) the randomly selected controllers all were MPC controllers.

Now the halgorithm is tasked with pushing a single object toward a target configuration. Except for the number of subtasks all parameters that determine the random environment will remain as

previously set for the random driving task.

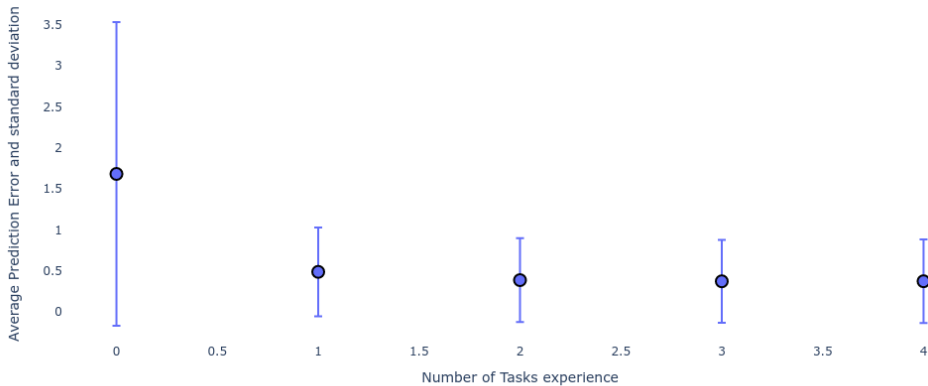


Figure 4.5: Average Prediction Error and Standard Deviation for action edges during a pushing task.

Martijn: averaged over how many experiments? related to that 1.5 and 2

The MPPI controller with *nonlinear-push-model-1* has an average PE between 1.5 and 2 and can be seen in the figure above as the most left data point in the prediction error plot. The same controller with *nonlinear-push-model-2* has an average lower PE between 0.4 and 0.6 and can be seen in the following data points (1, 2, 3 and 4). The *success factor*

Corrado: unclear how suc factor is defines, How exactly... put a reference to the formula number

is calculated based on the average prediction error so it is expected that the kgraph suggests the controller with the lower prediction error. It is expected that the PE goes down, which is exactly what Figure 4.5 shows. The halgorithm tests both edge parameterisations to conclude that the MPPI controller and *nonlinear-push-model-2* is the better of the two.

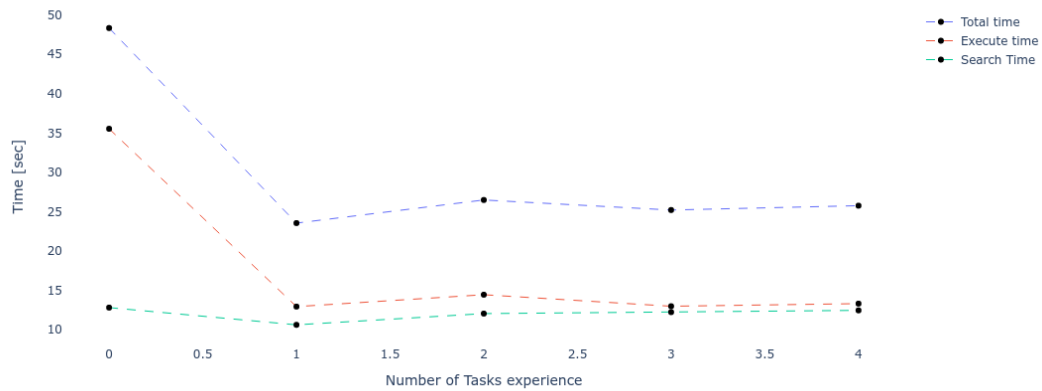


Figure 4.6: Planning times for pushing an object toward the target a configuration.

Corrado: A plot should be self contained, but there is no mention to the models used and there is no way to see that for myself from the graph

The MPPI controller with *nonlinear-push-model-2* does not only have a lower PE but is also faster compared to the MPPI controller combined with *nonlinear-push-model-1*. Execution time for driving toward the object and pushing that object to its target location takes around 15 seconds, with a search time to find that hypothesis being between 10 to 15 seconds. The result is that task execution time lowers, bear in mind that this result has to be taken with a grain of salt because the execution time is correlated with the path length (how far the object is from the robot, and how far should the object be pushed). It is better to look at the figure below that displays the execution time of both solving the same task with help of the kgraph and without its help.

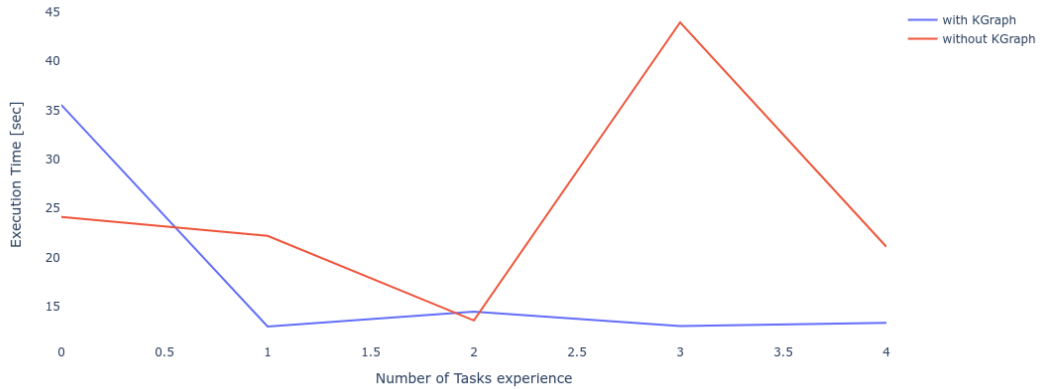


Figure 4.7: Execution times for pushing an object to target configurations with and without kgraph.

The kgraph suggestion work in favour of the execution time as can be seen in the Figure 4.7. Noticeable is that a random selection by pure chance selects the best choice of the controller as can be seen in 2 tasks of experience in the figure above.

4.3. Comparison with State-of-the-Art

Corrado: This should be structured better, it is an important part

In the introduction Table 1.1 was presented. A table that mainly shows which subset of the 3 main topics are included in which scientific paper. The 3 topics are learning system models, the NAMO problem and nonprehesile pushing. The table is presented again with the addition of the main testing method that is used by the state-of-the-art paper.

Author	Citation	Learns object dynamics	NAMO	Specify object target positions	Object Manipulation	test metric
Ellis et al.	[11]	✓	✓	✗	pushing	<u>success rate</u>
Sabbagh Novin et al.	[30]	✓	✗	✓	grasp-push grasp-pull	success rate, <u>execution time</u> prediction error, final position error
Scholz et al.	[31]	✓	✓	✗	graph-push grasp-pull	runtime, planning time, <u>number of calls to planner</u> number of calls to update model
Vega-Brown and Roy	[38]	✗	✓	✓	gripping	<u>computation time</u>
Wang et al.	[40]	✓	✓	✗	pushing	<u>computation and execution time</u>
Groote	proposed solution	✗/✓	✓	✓	pushing	see Table 4.1

Table 4.3: Overview of recent state-of-the-art papers that include a subset of the 3 topics (learning system models, NAMO, and nonprehensile pushing). The *grasp-push* and *grasp-pull* refer to prehensile push and pull manipulation, *gripped* refers to fully gripping and lifting objects for manipulation, *pushing* refers to nonprehensile push manipulation. The test metric indicates the testing method used by the paper, where the underlined metric is used to compare against the proposed framework.

update this table with the table from waaaaay above

Comparing Success Rate Ellis et al. claims to push with a success rate

Corrado: perhaps elaborate on that 100 percent, how does ellis define that?

of a 100% [11]. The test environment that Ellis et al. has used is very similar to the random pushing task discussed in Section 4.2. For both the random driving task and the random pushing task the success rate is 100%. Meaning that every driving or pushing subtask was successfully completed. It is even so that for the result of the random push task (displayed in Figures 4.5 to 4.7) the number of hypotheses is equal to the number of subtasks

Corrado: How do I see this? unclear to the reader

. Meaning that every subtask is completed by the first hypothesis generated. Both similar experiments from Ellis et al. and this thesis have a 100% success rate for similar , allowing us to conclude that the results are comparable.

Comparing Computation and Execution Time Three state-of-the-art papers that use computation and execution time as the testing metrics are compared to the proposed framework. To accomplish a fair comparison the environments that have been used in the

Corrado: Where do I see this?

citations are rebuilt in the pybullet software. The results are then directly compared to conclude that the proposed framework is as good as or even better in terms of computation time and execution time for similar tasks.

Wang et al. drives toward a target configuration that is blocked by a chair.

Corrado: By Wang or you?

The task is performed 3 times where the robot may remember its interactions with the chair from previous runs. The task is successfully completed all three times with a total time of 200 seconds for the first run to 180 seconds for the third run. Execution time increased from 70 to 85 seconds during these runs

Corrado: Why?

. Even with increasing execution times, the solution is found faster because the experience from previous runs could be used that lowered search time [40]. To compare against these results the environment is recreated in the pybullet software

Corrado: Show the recreated env then!

. The proposed framework was run only once, during this run it classified a wall object as unmovable, and the pushable box object with dimensions equal to that of the chair was classified as movable and moved out of the way. Overall execution time was 45 seconds whilst computation time took 65 seconds. The proposed framework successfully completed this similar task whilst having a lower computation and execution time. This allows concluding that the proposed framework improves upon the paper from Wang et al. with a decent margin.

Corrado: Put a screenshot side by side of your environment and Wang one

Vega-Brown and Roy has a task that pushes two boxes into a goal region. It takes around 300 seconds to return a hypothesis [38].

Corrado: What do you mean? for the next sentce

Both pushing tasks can be compared with two separate pushing tasks from the random push environment. By doubling the time to push a single object to its target configuration, $2 \cdot 30 = 60$ seconds both tasks could be compared. However, the point of Vega-Brown and Roy paper is that a global minimal task is sought. The proposed framework randomly selects a subtask and tries to complete it to then move to the next randomly selected subtask. A global minimum is thus not sought and both papers can therefore not be compared properly.

Corrado: Then why including it in the comparison?

Sabbagh Novin et al. grasp-pushes and grasp-pulls a walker object to two new target configurations [30]. The task is mimicked by pushing a box object of equal dimensions to the same target configurations. Compared to Sabbagh Novin et al. average of 125 and 160 seconds to complete task 1 and task 2 the proposed framework takes an average of only 27 and 33 seconds respectively (10 seconds computation time) to complete similar tasks. The decrease in total time allows to conclude that the proposed frameworks improve upon the method proposed by Sabbagh Novin et al.

Corrado: So your pushing controllers are performin better than prehensile manipulation? amazing, but doubt

Comparing Prediction Error Sabbagh Novin et al. displays the final position errors for a selection of objects which range from 0.05 to 0.6 meters. A success threshold is set to 0.1 meters, which determines that the object is at its target location [30]. The success threshold in this thesis is set to a staggering 0.9 meters,

Corrado: But then how can you compare success rate if you have different metrics for success?

thus it is concluded an object has reached its target position, whilst it is still 0.9 meters from its target configurations. This thesis does not try to reach optimal control, it tries to select the best controller in the available set of controllers. If the same controller from Sabbagh Novin et al. would be available, then similar final position errors would be obtained. It can be concluded that the prediction error

Corrado: Not position erro?

of the proposed framework is worse compared to this state-of-the-art. The reason is that the proposed framework focuses on improving the control selection and action sequences over time, and not on lowering final prediction errors.

5

Conclusions

This chapter answers the main and sub research questions. By referring to previously drawn conclusions and insights evidence is provided that supports the answers to the main and sub research questions.

Corrado: This part should be re structured according to the new research questions you'll have after addressing all comments. I'll give more feedback on the final conclusions in the version when available

First, the two research subquestions are answered. Recall first research subquestion:

"Can the proposed framework combine learning and planning for push en drive applications with a technique known as backward search?"

Chapter 3 is dedicated to presenting the proposed framework. It has been shown that the proposed framework that consists of the halgorithm, the hgraph and the kgraph work together can combine learning and planning with the technique of backward search. The proposed framework searches in the joint-configuration space.

Corrado: NExt senctende: What does this imply?

A search directly in composite space would result in the curse of dimensionality and is prevented by search only in a single mode of dynamics. Where a search is performed for a drive or push action. The hgraph is a graph-based structure that presents how the halgorithm is trying to complete a subtask. The structure of the hgraph is used to enforce the backward search technique, in which the halgorithm searches from the target configuration toward the start configuration. Newly gained environmental knowledge is stored in the kgraph, which firstly holds information on objects and if they can be manipulated, and secondly holds information on how they can be best manipulated. The kgraph can be filled with newly learned environmental knowledge and can be queried for action suggestions.

Recalling the second research subquestion, subquestion second research subquestion:

"Can the proposed framework combine learning and planning for push en drive applications? Can the proposed framework complete tasks, and how does it compare against the state-of-the-art?"

The proposed framework was able to perform as well, better or worse compared to the state-of-the-art, depending on which metric is taken into account. The proposed framework was tested against existing methods which only combine a subset of the 3 main topics that the proposed framework combines. The results discussed in Chapter 4 are compared to the state-of-the-art papers in Section 4.3. Five state-of-the-art papers are used to compare against the proposed framework. In the comparison success rate, planning time, execution time and several calls to the planner are used to compare. From the results, it can be concluded that the proposed framework learns relatively fast (prediction error comparison with [40]). The proposed framework can complete all of its assigned subtasks, giving it a comparable

success rate to the state-of-the-art (success rate comparison with [11]). This thesis does not have small prediction errors or low final position errors, it can be seen that the prediction errors are worse compared to the state-of-the-art (final position errors comparison with [30]).

The proposed framework improves upon the state-of-the-art exactly in its field of focus, improving task execution over time. It has been shown to learn faster compared to the state-of-the-art. Especially when the same or similar task is given to solve multiple times. Execution and planning times are equal or improved compared to the state-of-the-art. Lastly, prediction errors and final position errors are mainly worse compared to the state-of-the-art, which can be improved by better-designed controllers and more accurate system models.

Recall the main research question.

"How do objects' system models learn by a nonprehensile manipulation robot during task execution improve global task planning?"

Martijn: This is not the same as the question in the introduction!

How do learned objects' system models improve global task planning for a robot with nonprehensile push manipulation abilities over time?

Martijn: what does that mean, "improve affordance"?

The main research question can be answered in multiple ways. Mostly because object system models and environmental knowledge improves task execution in multiple ways. A classification of an object that is movable or unmovable improves affordance. Probabilistic action sequences that involve pushing unmovable objects cannot occur when object classification is present. Some (not all) system constraints that are captured by the system model, find in Algorithm 1, line 33 the *reachabilityCheck* where the learned system model prevents the planner from creating an unfeasible path. Thus System models improve paths found by the motion or manipulation planner, this conclusion remains unproven since the evidence is not provided. Lastly, system models in combination with a controller (and edge parameterization) improve task execution in many metrics. For which evidence is proved for metrics prediction error and execution time in Chapter 4.

Martijn: Overall comment: I read the main question in the introduction, and then immediately switched to here to read the answer. I honestly cannot follow this text.

5.1. Future work

Possible extensions to the proposed framework and improvements on the proposed framework are grouped in this section.

5.1.1. Removing Assumptions

Every assumption taken in Chapter 1 serves to simplify the problem and to narrow the scope of this thesis. They can however all be removed. Starting with assumption **closed-world assumption**, without this assumption the proposed framework must be much more robust. The proposed framework can with the help of this assumption conclude many conclusions deterministically. Examples are the feedback on edges and the classification of an object as unmovable or movable. In real-world applications unmovable objects can become movable, to make the transition toward removing the closed-world assumption the proposed framework must be converted to a probabilistic variant.

Moving from simulation toward the real world must remove the **perfect object sensor assumption**. Sensors and sensor fusion is required to estimate the configuration of the robot itself and objects in the environment. A start is to test the proposed framework with noise added to the perfect sensor.

The **tasks are commutative assumption** assumption makes it possible to randomly select a subtask without influencing the feasibility of the task. Removing this assumption can require an additional

rearrangement algorithm [19] to be run to determine a feasible order of handling subtasks.

The **objects do not tip over assumption** prevents objects from tipping over, but at the same time limits the number of objects. There are many possibilities to handle tipped objects. First, adding a tipping detector can detect when an object has tipped over. Then the proposed framework can threaten the objects as a new object and reclassify it. Another method would be a dedicated subroutine to place it in an upright position.

system identificaiton instead of hard-coded models

Glossary

List of Acronyms

MPPI Model Predictive Path Integral	ii
MPC Model Predictive Control	ii
NAMO Navigation Among Movable Objects	i
NP-hard non-deterministic polynomial-time hard	3
NP non-deterministic polynomial-time	65
FSM Finite State Machine	28
halgorithm hypothesis algorithm	iii
hgraph hypothesis graph	iii
kgraph knowledge graph	iii
IO Input-Output	10
PE Prediction Error	23
TE Tracking Error	23
RRT Rapidly-exploring Random Tree	
RRT* optimised Rapidly-exploring Random Tree	15
PRM Probabilistic Road Map	
PRM* optimised Probabilistic Road Map	
LTI Linear Time-Invariant	11
DOF Degrees Of Freedom	4
MDP Markov Decision Process	5

References

- [1] Ian Abraham et al. "Model-Based Generalization Under Parameter Uncertainty Using Path Integral Control". In: *IEEE Robotics and Automation Letters* 5.2 (Apr. 2020), pp. 2864–2871. issn: 2377-3766, 2377-3774. doi: 10.1109/LRA.2020.2972836. url: <https://ieeexplore.ieee.org/document/8988215/> (visited on 01/31/2022).
- [2] Ermano Arruda et al. "Uncertainty Averse Pushing with Model Predictive Path Integral Control". In: *2017 IEEE-RAS 17th International Conference on Humanoid Robotics (Humanoids)*. 2017 IEEE-RAS 17th International Conference on Humanoid Robotics (Humanoids). Birmingham: IEEE, Nov. 2017, pp. 497–502. isbn: 978-1-5386-4678-6. doi: 10.1109/HUMANOIDS.2017.8246918. url: <http://ieeexplore.ieee.org/document/8246918/> (visited on 04/29/2022).
- [3] Maria Bauza, Francois R. Hogan, and Alberto Rodriguez. "A Data-Efficient Approach to Precise and Controlled Pushing". Oct. 9, 2018. arXiv: 1807.09904 [cs]. url: <http://arxiv.org/abs/1807.09904> (visited on 03/01/2022).
- [4] Dmitry Berenson et al. "Manipulation Planning on Constraint Manifolds". In: *2009 IEEE International Conference on Robotics and Automation*. 2009 IEEE International Conference on Robotics and Automation (ICRA). Kobe: IEEE, May 2009, pp. 625–632. isbn: 978-1-4244-2788-8. doi: 10.1109/ROBOT.2009.5152399. url: <http://ieeexplore.ieee.org/document/5152399/> (visited on 12/05/2022).
- [5] Long Chen et al. "A Fast and Efficient Double-Tree RRT*-Like Sampling-Based Planner Applying on Mobile Robotic Systems". In: *IEEE/ASME Transactions on Mechatronics* 23.6 (Dec. 2018), pp. 2568–2578. issn: 1083-4435, 1941-014X. doi: 10.1109/TMECH.2018.2821767. url: <https://ieeexplore.ieee.org/document/8329210/> (visited on 04/14/2022).
- [6] Lin Cong et al. "Self-Adapting Recurrent Models for Object Pushing from Learning in Simulation". July 27, 2020. arXiv: 2007.13421 [cs]. url: <http://arxiv.org/abs/2007.13421> (visited on 04/06/2022).
- [7] Erwin Coumans and Yunfei Bai. *PyBullet, a Python Module for Physics Simulation for Games, Robotics and Machine Learning*. 2016–2021. url: <http://pybullet.org>.
- [8] E. W. Dijkstra. "A Note on Two Problems in Connexion with Graphs". In: *Numerische Mathematik* 1.1 (Dec. 1959), pp. 269–271. issn: 0029-599X, 0945-3245. doi: 10.1007/BF01386390. url: <http://link.springer.com/10.1007/BF01386390> (visited on 02/08/2023).
- [9] *Disjunctive Programming*. New York, NY: Springer Berlin Heidelberg, 2018. isbn: 978-3-030-00147-6.
- [10] Mohamed Elbanhawi and Milan Simic. "Sampling-Based Robot Motion Planning: A Review". In: *IEEE Access* 2 (2014), pp. 56–77. issn: 2169-3536. doi: 10.1109/ACCESS.2014.2302442. url: <https://ieeexplore.ieee.org/document/6722915/> (visited on 11/30/2022).
- [11] Kirsty Ellis et al. "Navigation among Movable Obstacles with Object Localization Using Photorealistic Simulation". In: July 2022. url: https://www.researchgate.net/publication/362092621_Navigation_Among_Movable_Obstacles_with_Object_Localization_using_Photorealistic_Simulation.
- [12] Hai-Ning Wu, M Levihn, and M Stilman. "Navigation Among Movable Obstacles in Unknown Environments". In: *2010 IEEE/RSJ International Conference on Intelligent Robots and Systems*. 2010 IEEE/RSJ International Conference on Intelligent Robots and Systems (IROS 2010). Taipei: IEEE, Oct. 2010, pp. 1433–1438. isbn: 978-1-4244-6674-0. doi: 10.1109/IROS.2010.5649744. url: <http://ieeexplore.ieee.org/document/5649744/> (visited on 05/06/2023).
- [13] Kris Hauser and Jean-Claude Latombe. "Multi-Modal Motion Planning in Non-expansive Spaces". In: *The International Journal of Robotics Research* 29.7 (June 2010), pp. 897–915. issn: 0278-3649, 1741-3176. doi: 10.1177/0278364909352098. url: <http://journals.sagepub.com/doi/10.1177/0278364909352098> (visited on 12/05/2022).

- [14] D. Hsu, J.-C. Latombe, and R. Motwani. "Path Planning in Expansive Configuration Spaces". In: *Proceedings of International Conference on Robotics and Automation*. International Conference on Robotics and Automation. Vol. 3. Albuquerque, NM, USA: IEEE, 1997, pp. 2719–2726. ISBN: 978-0-7803-3612-4. doi: 10.1109/ROBOT.1997.619371. url: <http://ieeexplore.ieee.org/document/619371/> (visited on 05/03/2023).
- [15] Sertac Karaman and Emilio Frazzoli. "Sampling-Based Algorithms for Optimal Motion Planning". In: *The International Journal of Robotics Research* 30.7 (June 2011), pp. 846–894. issn: 0278-3649, 1741-3176. doi: 10.1177/0278364911406761. url: <http://journals.sagepub.com/doi/10.1177/0278364911406761> (visited on 03/15/2022).
- [16] Eliahu Khalastchi and Meir Kalech. "On Fault Detection and Diagnosis in Robotic Systems". In: *ACM Computing Surveys* 51.1 (Jan. 31, 2019), pp. 1–24. issn: 0360-0300, 1557-7341. doi: 10.1145/3146389. url: <https://dl.acm.org/doi/10.1145/3146389> (visited on 12/13/2022).
- [17] Zachary Kingston, Mark Moll, and Lydia E. Kavraki. "Sampling-Based Methods for Motion Planning with Constraints". In: *Annual Review of Control, Robotics, and Autonomous Systems* 1.1 (May 28, 2018), pp. 159–185. issn: 2573-5144, 2573-5144. doi: 10.1146/annurev-control-060117-105226. url: <https://www.annualreviews.org/doi/10.1146/annurev-control-060117-105226> (visited on 05/06/2022).
- [18] Marek Kopicki et al. "Learning Modular and Transferable Forward Models of the Motions of Push Manipulated Objects". In: *Autonomous Robots* 41.5 (June 2017), pp. 1061–1082. issn: 0929-5593, 1573-7527. doi: 10.1007/s10514-016-9571-3. url: <http://link.springer.com/10.1007/s10514-016-9571-3> (visited on 03/15/2022).
- [19] Athanasios Krontiris and Kostas Bekris. "Dealing with Difficult Instances of Object Rearrangement". In: July 2015. doi: 10.15607/RSS.2015.XI.045.
- [20] Steven Michael LaValle. *Planning Algorithms*. Cambridge ; New York: Cambridge University Press, 2006. 826 pp. isbn: 978-0-521-86205-9.
- [21] Tekin Mericli, Manuela Veloso, and H. Levent Akin. "Push-Manipulation of Complex Passive Mobile Objects Using Experimentally Acquired Motion Models". In: *Autonomous Robots* 38.3 (Mar. 2015), pp. 317–329. issn: 0929-5593, 1573-7527. doi: 10.1007/s10514-014-9414-z. url: <http://link.springer.com/10.1007/s10514-014-9414-z> (visited on 01/31/2022).
- [22] neuromorphic tutorial. *LTC21 Tutorial MPPI*. June 7, 2021. url: https://www.youtube.com/watch?v=19QLyMuQ_BE (visited on 05/31/2022).
- [23] Roya Sabbagh Novin et al. "Dynamic Model Learning and Manipulation Planning for Objects in Hospitals Using a Patient Assistant Mobile (PAM)Robot". In: *2018 IEEE/RSJ International Conference on Intelligent Robots and Systems (IROS)*. 2018 IEEE/RSJ International Conference on Intelligent Robots and Systems (IROS). Madrid: IEEE, Oct. 2018, pp. 1–7. ISBN: 978-1-5386-8094-0. doi: 10.1109/IROS.2018.8593989. url: <https://ieeexplore.ieee.org/document/8593989/> (visited on 05/05/2022).
- [24] Manoj Pokharel. "Computational Complexity Theory(P,NP,NP-Complete and NP-Hard Problems)". In: (June 2020).
- [25] Philip Polack et al. "The Kinematic Bicycle Model: A Consistent Model for Planning Feasible Trajectories for Autonomous Vehicles?" In: *2017 IEEE Intelligent Vehicles Symposium (IV)*. 2017 IEEE Intelligent Vehicles Symposium (IV). Los Angeles, CA, USA: IEEE, June 2017, pp. 812–818. isbn: 978-1-5090-4804-5. doi: 10.1109/IVS.2017.7995816. url: <http://ieeexplore.ieee.org/document/7995816/> (visited on 05/03/2023).
- [26] James Rawlings, David Mayne, and Moritz Diehl. *Model Predictive Control: Theory, Computation and Design*. 2nd edition. Santa Barbara: Nob Hill Publishing, LLC, 2020. isbn: 978-0-9759377-5-4.
- [27] John Reif and Micha Sharir. "Motion Planning in the Presence of Moving Obstacles". In: *26th Annual Symposium on Foundations of Computer Science (Sfcs 1985)*. 26th Annual Symposium on Foundations of Computer Science (Sfcs 1985). Portland, OR, USA: IEEE, 1985, pp. 144–154. isbn: 978-0-8186-0644-1. doi: 10.1109/SFCS.1985.36. url: <http://ieeexplore.ieee.org/document/4568138/> (visited on 05/05/2022).

- [28] Nicholas Roy. "Hierarchy, Abstractions and Geometry". May 6, 2021. URL: <https://www.youtube.com/watch?v=mP-uK1PFqfI> (visited on 05/03/2023).
- [29] Roya Sabbagh Novin, Mehdi Tale Masouleh, and Mojtaba Yazdani. "Optimal Motion Planning of Redundant Planar Serial Robots Using a Synergy-Based Approach of Convex Optimization, Disjunctive Programming and Receding Horizon". In: *Proceedings of the Institution of Mechanical Engineers, Part I: Journal of Systems and Control Engineering* 230.3 (Mar. 2016), pp. 211–221. ISSN: 0959-6518, 2041-3041. doi: [10.1177/0959651815617883](https://doi.org/10.1177/0959651815617883). URL: <http://journals.sagepub.com/doi/10.1177/0959651815617883> (visited on 05/05/2022).
- [30] Roya Sabbagh Novin et al. "A Model Predictive Approach for Online Mobile Manipulation of Non-Holonomic Objects Using Learned Dynamics". In: *The International Journal of Robotics Research* 40.4-5 (Apr. 2021), pp. 815–831. ISSN: 0278-3649, 1741-3176. doi: [10.1177/0278364921992793](https://doi.org/10.1177/0278364921992793). URL: <http://journals.sagepub.com/doi/10.1177/0278364921992793> (visited on 05/05/2022).
- [31] Jonathan Scholz et al. "Navigation Among Movable Obstacles with Learned Dynamic Constraints". In: *2016 IEEE/RSJ International Conference on Intelligent Robots and Systems (IROS)*. 2016 IEEE/RSJ International Conference on Intelligent Robots and Systems (IROS). Daejeon, South Korea: IEEE, Oct. 2016, pp. 3706–3713. ISBN: 978-1-5090-3762-9. doi: [10.1109/IROS.2016.7759546](https://doi.org/10.1109/IROS.2016.7759546). URL: <http://ieeexplore.ieee.org/document/7759546/> (visited on 04/29/2022).
- [32] Neal Seigmiller et al. "Vehicle Model Identification by Integrated Prediction Error Minimization". In: *The International Journal of Robotics Research* 32.8 (July 2013), pp. 912–931. ISSN: 0278-3649, 1741-3176. doi: [10.1177/0278364913488635](https://doi.org/10.1177/0278364913488635). URL: <http://journals.sagepub.com/doi/10.1177/0278364913488635> (visited on 02/16/2022).
- [33] Max Spahn. *Urdf-Environment*. Version 1.2.0. Aug. 8, 2022. URL: https://github.com/maxspahn/gym_envs_urdf.
- [34] Jochen Stüber, Marek Kopicki, and Claudio Zito. "Feature-Based Transfer Learning for Robotic Push Manipulation". In: *2018 IEEE International Conference on Robotics and Automation (ICRA)* (May 2018), pp. 5643–5650. doi: [10.1109/ICRA.2018.8460989](https://doi.org/10.1109/ICRA.2018.8460989). arXiv: [1905.03720](https://arxiv.org/abs/1905.03720). URL: <http://arxiv.org/abs/1905.03720> (visited on 03/15/2022).
- [35] Jochen Stüber, Claudio Zito, and Rustam Stolkin. "Let's Push Things Forward: A Survey on Robot Pushing". In: *Frontiers in Robotics and AI* 7 (Feb. 6, 2020), p. 8. ISSN: 2296-9144. doi: [10.3389/frobt.2020.00008](https://doi.org/10.3389/frobt.2020.00008). arXiv: [1905.05138](https://arxiv.org/abs/1905.05138). URL: <http://arxiv.org/abs/1905.05138> (visited on 02/24/2022).
- [36] Marc Toussaint et al. "Sequence-of-Constraints MPC: Reactive Timing-Optimal Control of Sequential Manipulation". Mar. 10, 2022. arXiv: [2203.05390 \[cs\]](https://arxiv.org/abs/2203.05390). URL: <http://arxiv.org/abs/2203.05390> (visited on 04/29/2022).
- [37] Jur van den Berg et al. "Path Planning among Movable Obstacles: A Probabilistically Complete Approach". In: *Algorithmic Foundation of Robotics VIII*. Ed. by Gregory S. Chirikjian et al. Red. by Bruno Siciliano, Oussama Khatib, and Frans Groen. Vol. 57. Berlin, Heidelberg: Springer Berlin Heidelberg, 2009, pp. 599–614. ISBN: 978-3-642-00311-0 978-3-642-00312-7. doi: [10.1007/978-3-642-00312-7_37](https://doi.org/10.1007/978-3-642-00312-7_37). URL: http://link.springer.com/10.1007/978-3-642-00312-7_37 (visited on 06/24/2022).
- [38] William Vega-Brown and Nicholas Roy. "Asymptotically Optimal Planning under Piecewise-Analytic Constraints". In: *Algorithmic Foundations of Robotics XII*. Ed. by Ken Goldberg et al. Vol. 13. Cham: Springer International Publishing, 2020, pp. 528–543. ISBN: 978-3-030-43088-7 978-3-030-43089-4. doi: [10.1007/978-3-030-43089-4_34](https://doi.org/10.1007/978-3-030-43089-4_34). URL: http://link.springer.com/10.1007/978-3-030-43089-4_34 (visited on 06/23/2022).
- [39] M. Verhaegen and Vincent Verdult. *Filtering and System Identification: A Least Squares Approach*. Cambridge ; New York: Cambridge University Press, 2007. 405 pp. ISBN: 978-0-521-87512-7.
- [40] Maozhen Wang et al. "Affordance-Based Mobile Robot Navigation Among Movable Obstacles". In: *2020 IEEE/RSJ International Conference on Intelligent Robots and Systems (IROS)*. 2020 IEEE/RSJ International Conference on Intelligent Robots and Systems (IROS). Las Vegas, NV, USA: IEEE, Oct. 24, 2020, pp. 2734–2740. ISBN: 978-1-72816-212-6. doi: [10.1109/IROS45743.2020.9341337](https://doi.org/10.1109/IROS45743.2020.9341337). URL: <https://ieeexplore.ieee.org/document/9341337/> (visited on 06/28/2022).

- [41] Grady Williams, Andrew Aldrich, and Evangelos Theodorou. "Model Predictive Path Integral Control Using Covariance Variable Importance Sampling". Oct. 28, 2015. arXiv: 1509.01149 [cs]. URL: <http://arxiv.org/abs/1509.01149> (visited on 05/02/2022).
- [42] Liangjun Zhang, Young J. Kim, and Dinesh Manocha. "A Simple Path Non-existence Algorithm Using C-Obstacle Query". In: *Algorithmic Foundation of Robotics VII*. Ed. by Srinivas Akella et al. Vol. 47. Berlin, Heidelberg: Springer Berlin Heidelberg, 2008, pp. 269–284. ISBN: 978-3-540-68404-6 978-3-540-68405-3. doi: 10.1007/978-3-540-68405-3_17. URL: http://link.springer.com/10.1007/978-3-540-68405-3_17 (visited on 06/16/2022).

6

Appendix

The appendix contains additional information that may help better understand the thesis.

A

Complexity Classes

Problems in class P have a solution which can be found in polynomial time, problems in non-deterministic polynomial-time (NP) are problems for which no polynomial algorithms have been found yet, and of which it is believed that no polynomial time solution exist. For problems in NP, when provided with a solution, verifying that the solution is indeed a valid solution can be done in polynomial time. NP-hard problems are a class of problems which are at least as hard as the hardest problems in NP. Problems that are NP-hard do not have to be elements of NP. They may not even be decidable [24]. This thesis or other recent studies in the references do not attempt to find an optimal solution. Instead, they provide a solution whilst guaranteeing properties such as near-optimality or probabilistic completeness. As the piano's mover problem can be reduced to the NAMO problem combined with relocating objects to target positions, the conclusion can be drawn that this NAMO problem is NP-hard.

B

Control Methods

B.1. MPC Control

In recent literature involving predictive methods Model Predictive Control (MPC) methods are dominating, before moving on to MPC and variations of MPC, MPC will briefly be explained. The basic concept of MPC is to use a dynamic model to forecast system behaviour and optimise the forecast to produce the best decision for the control move at the current time. Models are therefore central to every form of MPC. Because the optimal control move depends on the initial state of the dynamic system [26]. A dynamical model can be presented in various forms, let's consider a familiar differential equation.

$$\begin{aligned}\frac{dx}{dt} &= f(x(t), u(t)) \\ y &= h(x(t), u(t)) \\ x(t_0) &= x_0\end{aligned}$$

In which $x \in \mathbb{R}^n$ is the state, $u \in \mathbb{R}^m$ is the input, $y \in \mathbb{R}^p$ is the output, and $t \in \mathbb{R}$ is time. The initial condition specifies the value of the state x at $t = t_0$, and a solution to the differential equation for time greater than t_0 , $t \in \mathbb{R}_{\geq 0}$ is sought. If little knowledge about the internal structure of a system is available, it may be convenient to take another approach where the state is suppressed, no internal structure about the system is known and the focus lies only on the manipulable inputs and measurable outputs. As shown in figure B.1, consider the system $G(t)$ to be the connection between u and y . In this viewpoint, various system identification techniques are used, in which u is manipulated and y is measured [26]. From the input-output relation, a system model is estimated or improved. The system model can be seen inside the MPC controller block in figure B.1.

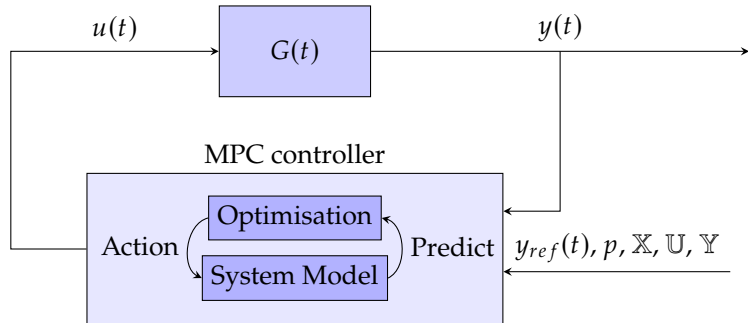


Figure B.1: System $G(t)$ with input $u(t)$, output $y(t)$ and MPC controller with input $y(t)$, reference signal $y_{ref}(t)$, parameterisation p and constraint sets $\mathbb{X}, \mathbb{U}, \mathbb{Y}$

Some states of the system might be inside an obstacle region, such a region is undesirable for the robot to be in or go toward. The robot states are allowed in free space, which is all space minus the

obstacle region. The free space is specified as a state constrained set \mathbb{X} . Allowable input can be restricted by the input constraint set \mathbb{U} , a scenario in which input constraints are required is for example the maximum torque an engine produces at full throttle. Lastly, the set of allowed outputs is specified in the output constraint set \mathbb{Y} . State, input and output constraints must be respected during optimisation, the optimiser takes the state-, input- and output constraint sets $\mathbb{X}, \mathbb{U}, \mathbb{Y}$ and if feasible, finds an action sequence driving the system toward the reference signal while constraints are respected. The MPC system model predicts future states where the system is steered toward as a result of input actions.

The optimisation minimises an objective function $V_N(x_0, y_{ref}, \mathbf{u}_N(0))$, where $\mathbf{u}_N(k) = (u_k, u_{k+1}, \dots, u_{k+N})$. The objective function takes the reference signal as an argument together with the initial state and the control input for the control horizon. The objective function then creates a weighted sum of some heuristic function. States and inputs resulting in outputs far from the reference signal are penalised more by the heuristic function than outputs closer to the reference signal. Because the objective function is a Lyapunov function, it has the property that, it has a global minimum for the optimal input \mathbf{u}_N^* . If the system output reaches the reference signal y_{ref}, x_{ref} then u_{ref} will be mapped to the output reference signal as such $y_{ref} = h(x_{ref}, u_{ref})$. As a result solving the minimisation problem displayed in equation (B.1) gives the optimal input which steers the system toward the output reference signal while at the same time respecting the constraints.

$$\begin{aligned} & \underset{u_k, u_{k+1}, \dots, u_{k+N}}{\text{minimize}} && V_N(x_0, y_{ref}, u_k, u_{k+1}, \dots, u_{k+N}) \\ & \text{subject to} && x(k+1) = f(x(k), u(k)), \\ & && x \in \mathbb{X}, \\ & && u \in \mathbb{U}, \\ & && y \in \mathbb{Y}, \\ & && x(0) = x_0 \end{aligned} \tag{B.1}$$

Figure B.2 displays the predicted output converging toward the constant output reference. After solving the minimisation problem, equation (B.1), the optimal input sequence is obtained \mathbf{u}_N^* (given that the constraints are respected for such input), from which only the first input is executed for time step k to $k + 1$. Then all indices are shifted such that the previous time step $k + 1$ becomes k , the output is measured and the reference signal, parameterisation, and constraints sets are updated and a new minimisation problem is created, which completes the cycle. Note that figures B.1 and B.2 is an example MPC controller, which hardly scratched the surface of MPC, there are many variations and additions such as deterministic and stochastic MPC, stage and terminal cost, distributed MPC, etc. which [26] visits extensively.

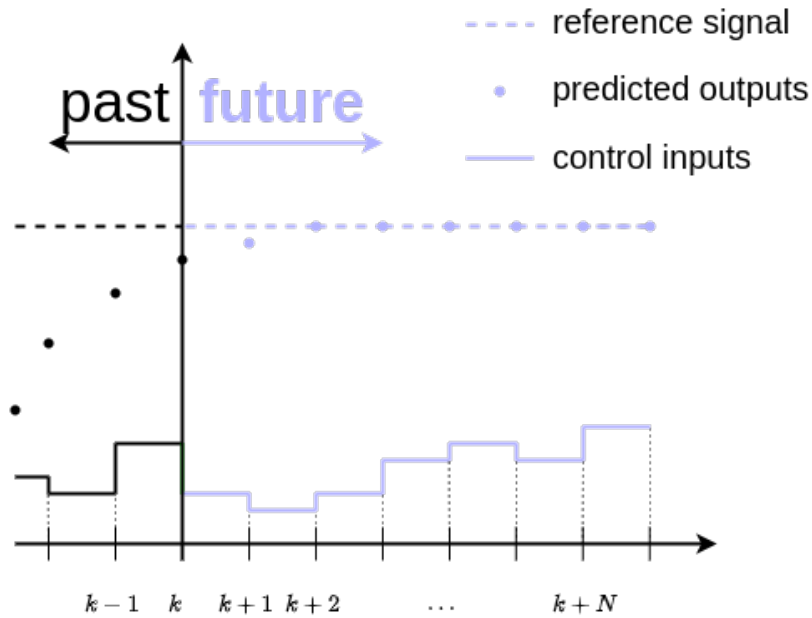


Figure B.2: A discrete MPC scheme tracking a constant reference signal. k indicates the discrete time step, N the control horizon

B.2. MPPI Control

Introduced by [41] MPPI control arose. Which was followed by MPPI control combined with various system models, identification methods [1, 6, 2]. The core idea is from the current state of the system with the use of a system model and randomly sampled inputs to simulate in the future a number of "rollouts" for a specific time horizon, [22]. These rollouts indicate the future states of the system if the randomly sampled inputs would be applied to the system, the future states can be evaluated by a cost function which penalised undesired states and rewards desired future states. A weighted sum over all rollouts determines the input which will be applied to the system. If a goal state is not reached, the control loop starts with the next iteration. An example is provided, see figure B.3.

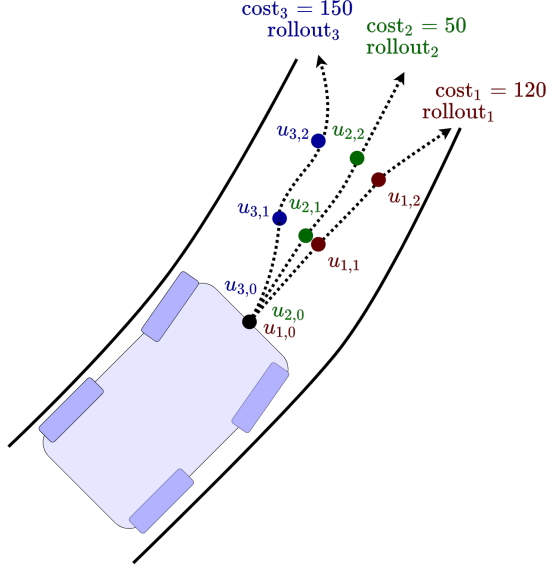


Figure B.3: MPPI controlled race car using a control horizon of 3 time steps, with 3 rollouts all having their respected inputs as $u_{i,j}$ where i is the rollout index and j indicates the time step [22].

Here 3 rollouts are displayed, The objective function is designed to keep the car driving on the center of the road by penalising rollouts which are further away from the center of the road relatively more. resulting in a high cost for rollout₁ and rollout₃ compared to rollout₂. As a result, the input send to the system as a weighted sum of the rollouts is mostly determined by rollout₂. The weighted sum determining the input is displayed in equation (B.2), from [22].

$$u(k+1) = u(k) + \frac{\sum_i w_i \delta u_i}{\sum_i w_i} \quad (\text{B.2})$$

Where δu_i is the difference between $u(k)$ and the input for rollout i , the weight of rollout _{i} is determined as: $w_i = e^{-\frac{1}{\lambda} \text{cost}_i}$, λ is a constant parameter.